

UNCLASSIFIED

AD NUMBER
AD909213
NEW LIMITATION CHANGE
TO Approved for public release, distribution unlimited
FROM Distribution authorized to U.S. Gov't. agencies only; Test and Evaluation; MAR 1973. Other requests shall be referred to Army Missile Command, ATTN: AMSMI-RSM, Redstone Arsenal, AL 35809.
AUTHORITY
MICOM ltr dtd 24 Sep 1973

THIS PAGE IS UNCLASSIFIED

FINAL TECHNICAL REPORT  
Project A-1381

AN INVESTIGATION OF FUSED SILICA COMPOSITES FOR IMPROVEMENT  
OF ABLATION AND RAIN EROSION RESISTANCE, AND AN ALTERNATE  
METHOD FOR MANUFACTURE OF FUSED SILICA RADOMES

By  
E. A. Welsh, S. A. Byers, and J. N. Harris

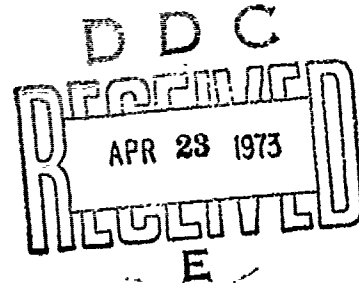
Contract DAAH01-72-C-0400

Prepared for  
U.S. Army Missile Command  
Redstone Arsenal, Alabama 35809

March 1973

Engineering Experiment Station  
Georgia Institute of Technology  
Atlanta, Georgia 30332

Distribution limited to U.S. Government agencies  
only; other requests for this document must be  
referred to U.S. Army Missile Command (AMSMI-RSM).



TVE  
23 APR 1973

AD 309213

FINAL TECHNICAL REPORT  
Project A-1381

AN INVESTIGATION OF FUSED SILICA COMPOSITES FOR IMPROVEMENT  
OF ABLATION AND RAIN EROSION RESISTANCE, AND AN ALTERNATE  
METHOD FOR MANUFACTURE OF FUSED SILICA RADOMES

By  
E. A. Welsh, S. A. Byers, and J. N. Harris

Contract DAAH01-72-C-0400

Prepared for  
U.S. Army Missile Command  
Redstone Arsenal, Alabama 35809

March 1973

Engineering Experiment Station  
Georgia Institute of Technology  
Atlanta, Georgia 30332

Distribution limited to U.S. Government agencies  
only; other requests for this document must be  
referred to U.S. Army Missile Command (AMSMI-RSM).

*TvE*  
23 APR 1973

## FOREWORD

This report was prepared by the Engineering Experiment Station of the Georgia Institute of Technology, Atlanta, Georgia 30332 under U. S. Army Contract DAAH01-72-C-0400.

The work under this program was conducted as two separate tasks. Task I was "An Investigation of Fused Silica Composites for Improvement of Ablation and Rain Erosion Resistance." Task II was "An Alternate Method for Manufacture of Fused Silica Radomes." Therefore, the report is divided into two sections. Section I is concerned with slip-cast fused silica composites. Section II discusses the isostatic pressing of fused silica powders.

Principal personnel engaged in work on this program were J. N. Harris, R. A. Arrieta, G. Boscoe, S. A. Byers, N. E. Poulos, J. D. Walton and E. A. Welsh. Authors of this report were E. A. Welsh, S. A. Byers, J. N. Harris, R. A. Arrieta and G. Boscoe.

## ABSTRACT

The objectives of this program are to develop composite materials based on slip-cast fused silica which have a higher degree of rain erosion resistance and ablation resistance than fused silica itself, and to develop a method other than slip casting for fabrication of rebonded fused silica radomes.

Task I of this program studied the effects of small additions of SiC and  $\text{Si}_3\text{N}_4$  on the ablation and rain erosion resistance of slip-cast fused silica. The best composites were in the range of 10 per cent SiC and 10 per cent  $\text{Si}_3\text{N}_4$ . Ablation resistance was improved with both additives, but resistance to rain erosion did not show any improvement under the test conditions used.

Task II of this program evaluated isostatic pressing as an alternate radome forming method. Radome shapes were pressed; however, physical properties of the pressed fused silica powders were less than those of slip-cast items. Work so far indicates that the isostatic pressing process has potential, but that further development is still needed.

TABLE OF CONTENTS

	Page
I. SLIP-CAST FUSED SILICA COMPOSITES . . . . .	1
A. Introduction . . . . .	1
1. Program and Objectives . . . . .	1
2. Program Goals . . . . .	1
3. Background . . . . .	1
B. Experimental Program . . . . .	5
1. Literature Survey . . . . .	5
2. Fused Silica Slip Characterization . . . . .	7
3. Composite Development . . . . .	8
a. Silicon Carbide Composites . . . . .	8
b. Silicon Nitride Composites . . . . .	29
c. Boron Nitride Composites . . . . .	32
4. Composite Characterization . . . . .	32
a. Physical and Mechanical Testing . . . . .	32
b. Electrical Testing . . . . .	33
c. Ablation Resistance Testing . . . . .	33
d. Rain Erosion Resistance Testing . . . . .	36
C. Discussion . . . . .	37
D. Conclusions . . . . .	38
E. Recommendations . . . . .	39
II. ISOSTATIC PRESSING OF FUSED SILICA . . . . .	41
A. Introduction . . . . .	41
1. Program and Objectives . . . . .	41
2. Program Goals . . . . .	41
B. Experimental Program . . . . .	42
1. Approach . . . . .	42

(Continued)

TABLE OF CONTENTS (Continued)

	Page
2. Program . . . . .	42
a. Initial Powder Evaluations . . . . .	42
b. Grain/Cab-0-Sil <sup>®</sup> Mixture Studies . . . . .	43
c. Initial Firing and Property Evaluation . . . . .	45
d. Powder Reevaluation . . . . .	47
e. Binder Evaluation . . . . .	53
f. Pressing Procedures . . . . .	53
g. Pressed Powder Evaluations . . . . .	54
h. Cab-0-Sil <sup>®</sup> Agglomeration . . . . .	56
i. Spray Drying . . . . .	57
j. High Purity Fused Silica Grain Mixtures . . . . .	63
k. Radome Tooling and Pressing . . . . .	66
C. Discussion . . . . .	68
1. Powder Preparation . . . . .	68
2. Spray Drying . . . . .	69
3. High Purity Fused Silica Grain . . . . .	69
4. Pressing of Radome Shapes . . . . .	69
D. Conclusions . . . . .	69
E. Author's Opinion of the Isostatic Process as an Alternative Forming Process for Fused Silica Radome Shapes . . . . .	70
F. Recommendations for Future Work . . . . .	71
III. APPENDIX . . . . .	73
I. SINTERING DATA FOR SILICON CARBIDE/SILICA COMPOSITES . . . . .	73
II. GRAPHICAL REPRESENTATION OF DENSITY AND SHRINKAGE VERSUS FIRING TIME (2300° F) FOR ISOSTATICALLY PRESSED POWDERS . . . . .	77

(Continued)

TABLE OF CONTENTS (Concluded)

	Page
III. MILLING OF HIGH PURITY FUSED SILICA (SYLVANIA) CULLET . . . . .	89
IV. PROCEDURE USED TO PRESS RADOME . . . . .	91
IV. REFERENCES . . . . .	93

## LIST OF ILLUSTRATIONS

	Page
1. Particle Size Distribution - High Purity Fused Silica Slip. . .	10
2. Particle Size Distributions - Silicon Carbide Powders . . . . .	12
3. Per Cent Theoretical Density Versus Sintering Time at 2300° F for Slip-Cast Fused Silica with 0 to 15 Per Cent Additions of Equal Parts Silicon Carbide A, C, and E . . . . .	16
4. Tensile Strength Versus Sintering Time at 2300° F for Slip-Cast Fused Silica with 0 to 15 Per Cent Additions of Equal Parts Silicon Carbide A, C, and E . . . . .	17
5. Sintering Data Versus Composition for 10 Per Cent SiC/SiO <sub>2</sub> Composites. . . . .	18
6. Calculated Particle Size Distribution and Best Fit Line for Composite Slip with 10 Per Cent Silicon Carbide Powder E. . . .	20
7. Packing Efficiency Versus Coefficient of Variance for SiC/SiO <sub>2</sub> Composites . . . . .	22
8. Particle Size Distributions of Maximum and Minimum Packing Efficiency, and Range of Size Distributions for Maximum Packing From Andreasen Relationship . . . . .	27
9. Particle Size Distribution for Silicon Nitride Powder . . . . .	30
10. Flow Sheet of Experimental Program for Development of Isostatically Pressed Fused Silica. . . . .	44
11. Ternary Packing Equilibrium Diagram for Fused Silica Grains . .	52
12. Scanning Electron Micrograph of Bowen Powders Containing 2 weight per cent Carbowax. . . . .	60
13. Scanning Electron Micrograph of Spray Dried Fused Silica Slip Collected at Georgia Tech. . . . .	61
14. Scanning Electron Micrograph of 90 weight per cent Silica from Ludox <sup>®</sup> - 10 per cent Cab-O-Sil <sup>®</sup> L-5. . . . .	62
15. Tooling Used to Isostatically Press Radome. . . . .	67
16a. Density Versus Sintering Time @ 2300° F . . . . .	78
16b. Density Versus Sintering Time @ 2300° F . . . . .	79
16c. Density Versus Sintering Time @ 2300° F . . . . .	80

LIST OF ILLUSTRATIONS (Continued)

	Page
16d. Density Versus Sintering Time @ 2300° F. . . . .	81
16e. Density Versus Sintering Time @ 2300° F. . . . .	82
17a. Shrinkage Versus Sintering Time @ 2300° F. . . . .	83
17b. Shrinkage Versus Sintering Time @ 2300° F. . . . .	84
17c. Shrinkage Versus Sintering Time @ 2300° F. . . . .	85
17d. Shrinkage Versus Sintering Time @ 2300° F. . . . .	86
17e. Shrinkage Versus Sintering Time @ 2300° F. . . . .	87

LIST OF TABLES

	Page
I. RELATIVE RAIN EROSION RESISTANCE OF CANDIDATE CERAMIC RADOME MATERIALS . . . . .	3
II. CHARACTERIZATION DATA ON THERMO MATERIALS FUSED SILICA SLIP 050972-2 . . . . .	9
III. CHEMICAL ANALYSIS OF THERMO MATERIALS SLIP 050972-2 . . . . .	9
IV. CHARACTERIZATION DATA ON 3/4-INCH DIAMETER CYLINDRICAL TEST SPECIMENS SLIP-CAST FROM THERMO MATERIALS SLIP 050972-2 AND SINTERED 5-1/2 HOURS AT 2210° F . . . . .	11
V. MEAN VALUES OF PROPERTIES OF SiO <sub>2</sub> -SiC COMPOSITES . . . . .	13
VI. DATA MATRIX FOR PACKING EFFICIENCY CORRELATION ANALYSIS . . . . .	23
VII. CORRELATION COEFFICIENT MATRIX PACKING EFFICIENCY STUDY . . . . .	24
VIII. REVISED CORRELATION COEFFICIENT MATRIX . . . . .	24
IX. DATA MATRIX FOR EFFECTS OF SLIP PROPERTIES ON SINTERING PROPERTIES AND TENSILE STRENGTH . . . . .	26
X. CORRELATION COEFFICIENT MATRIX FOR EFFECTS OF SLIP PROPERTIES ON SINTERING PROPERTIES AND TENSILE STRENGTH . . . . .	26
XI. EFFECT OF ADDITIVE VOLUME ON TENSILE STRENGTH . . . . .	28
XII. CORRELATION COEFFICIENT MATRIX ADDITIVE VOLUME EFFECTS . . . . .	28
XIII. SINTERING DATA FOR Si <sub>3</sub> N <sub>4</sub> COMPOSITES . . . . .	31
XIV. CHARACTERIZATION DATA ON FUSED SILICA COMPOSITES . . . . .	34
XV. DIELECTRIC CONSTANT & LOSS TANGENT FOR SiC/SiO <sub>2</sub> AND Si <sub>3</sub> N <sub>4</sub> /SiO <sub>2</sub> COMPOSITES . . . . .	35
XVI. MATERIAL PROPERTIES OF ISOSTATICALLY PRESSED FUSED SILICA TRIAL POWDERS . . . . .	46
XVII. RESULTS OF ISOSTATICALLY PRESSED FUSED SILICA GRAIN (POWDER E-F FROM TABLE I) . . . . .	48

(Continued)

LIST OF TABLES (Continued)

	Page
XVIII. SUMMARY OF BLENDS . . . . .	49
XIX. PACKING DENSITY OF VARIOUS GRAIN SIZE DISTRIBUTIONS . . . . .	51
XX. MATERIAL PROPERTIES OF ISOSTATICALLY PRESSED FUSED SILICA POWDERS WITH INCREASING CAB-O-SIL <sup>®</sup> CONTENT . . . . .	55
XXI. TRIALS MADE WITH THE EES LABORATORY SPRAY DRYER . . . . .	58
XXII. ISOSTATICALLY PRESSED HIGH PURITY FUSED SILICA GRAIN MIXTURES . . . . .	64
XXIII. COMPARATIVE SPECTROGRAPHIC ANALYSES OF PRESSED HIGH PURITY GRAIN AND SLIP-CAST FUSED SILICA . . . . .	65
XXIV. SINTERING DATA FOR SILICON CARBIDE/SILICA COMPOSITES . . . . .	74

SECTION I  
SLIP-CAST FUSED SILICA COMPOSITES

A. Introduction

1. Program and Objectives

The objective of work carried out under this phase of Contract DAAH01-72-C-0400 was to produce optimal slip-cast fused silica composites having better rain erosion and ablation resistance than unmodified slip-cast fused silica. Previous efforts have demonstrated that silicon carbide and silicon nitride additives have improved ablation resistance of slip-cast fused silica. The program will concentrate on these materials.

2. Program Goals

The goals of the program were outlined as follows:

- a) To study the effects of particle size distribution on packing efficiency and tensile strength of composite materials.
- b) To obtain maximum tensile strength for composite materials by optimizing casting and sintering conditions.
- c) To evaluate the relative ablation and rain erosion resistance of selected composite materials.

3. Background

Slip-cast fused silica is one of a very few materials suitable for radome applications above Mach 5. Its excellent thermal shock

resistance, stable dielectric properties with respect to changes in temperature and frequency, and low thermal conductivity are unequaled by any other material. However, there is a need for improvement of slip-cast fused silica in the areas of ablation and rain erosion resistance.

Unlike most other ceramic materials fused silica does not have a true melting point that is sharply defined by a sudden rapid decrease in viscosity. The generally quoted melting temperature is that defined as softening point of glasses and corresponds to a viscosity of  $10^{7.6}$  poise. This viscosity is reached at a temperature of approximately  $3110^{\circ}$  F. Above this temperature the viscosity of fused silica continues to decrease slowly and is still greater than  $10^4$  poise at  $4500^{\circ}$  F.

For certain high temperature applications where low shear is involved, fused silica may be used at temperatures above its stated melting point. However, radomes operating above Mach 5 are subject to high temperature and high shear. This could cause a deformation of the silica due to plastic flow or under more severe conditions could cause a stripping away of the surface layers.

One of the advantages of slip-cast fused silica radomes is their low cost compared to other ceramic radomes. Slip-casting is a low-cost method of fabrication and final dimensions are easily obtained by machining with diamond grinding wheels. The relative softness of the slip-cast material speeds up the machining process but is a detriment to rain erosion resistance. A ranking of rain erosion resistance for candidate ceramic radome materials for use above Mach 5 is shown in the following table.

TABLE I  
RELATIVE RAIN EROSION RESISTANCE OF CANDIDATE CERAMIC  
RADOME MATERIALS

<u>Good</u>	<u>Fair</u>	<u>Poor</u>
$Al_2O_3$	Pyroceram 9606	SCFS
BeO	Rayceram III	IPBN

Although the rain erosion and ablation resistance of slip-cast fused silica radomes is satisfactory for current applications it needs to be improved for future requirements.

In improving rain erosion and ablation resistance it is important not to degrade the dielectric, thermal shock and thermal conductivity properties of the slip-cast fused silica. One method of accomplishing this is by the addition of small quantities of very refractory and very hard materials which will not react chemically with the silica. It has been shown by Kingery 1/ and others that the addition of small quantities of material to a major phase has very little effect on properties such as thermal conductivity and dielectric constant. However, small additions of refractory material could make the silica more viscous and less likely to flow under high temperature and high shear. It could also prevent the propagation of surface cracks in the silica caused by high velocity impact with rain or other materials.

Past attempts to use fibrous refractory materials for these purposes 2/ have proven unsatisfactory due to packing problems in slip-casting and the inability to increase the density on sintering.

Because of these problems the use of particulate materials was investigated. A wide range of very refractory materials was investigated 3/; however, some of these materials were much denser than fused silica and problems occurred in obtaining homogeneous samples while using slip-casting techniques. Further experience on the same program has indicated that improved ablation and impact resistance is achieved when small additions of silicon carbide and silicon nitride powders are added to the fused silica slip. These particles do not dissolve into the fused silica but are retained as a discrete phase in the fused silica matrix.

Three refractory additives appear promising for increasing ablation and/or rain erosion resistance of slip-cast fused silica. These are: boron nitride (BN), silicon carbide (SiC) and silicon nitride ( $\text{Si}_3\text{N}_4$ ).

Boron nitride has a much higher heat of ablation than does fused silica; hence, combining boron nitride powder with fused silica slip should result in a composite material with improved ablation properties. Boron nitride, like fused silica, has a relatively low rain erosion resistance; therefore, it is not expected that any improvement in rain erosion resistance will be achieved with  $\text{SiO}_2/\text{BN}$  composites. The dielectric constant and the density of BN are relatively close to that of fused silica so there should be no problems with settling of the BN out of the slip, and there should be no great changes in effective dielectric constant of the composite.

Composites of slip-cast fused silica and silicon carbide have been prepared at Georgia Tech which show some improvement over slip-cast fused silica in both resistance to impact and resistance to ablation. The density of silicon carbide is relatively close to the density of fused silica, so no settling problems occur in slip

casting composites. Unfortunately, technical grade silicon carbide is an electrical conductor and may restrict  $\text{SiO}_2/\text{SiC}$  composites to non-electrical uses such as nose tips and leading edges. The higher purity grades of SiC have higher resistances and composites made with these grade may have satisfactory dielectric properties for radome use; however, this can only be determined by experiment.

Silicon nitride has hardness and other properties similar to silicon carbide and in addition has good dielectric properties. It is expected that silicon nitride in a fused silica composite would act very similarly to silicon carbide. A  $\text{SiO}_2/\text{Si}_3\text{N}_4$  composite should also have dielectric properties very similar to slip-cast fused silica since the dielectric constant of  $\text{Si}_3\text{N}_4$  is only slightly higher than that of fused silica.

## B. Experimental Program

### 1. Literature Survey

A literature survey was carried out to determine what, if any, literature was available on the relationship between particle size distributions of slips and the bulk densities of castings. Many studies have been made of packing of sized spheres and of dry powders, but relatively little information was found on slip casting.

The most frequently cited relationship was the empirical Andreasen equation 4/, 5/ which states that in order to obtain maximum packing density in a slip-cast material, the particle size distribution of the casting slip must fall within the range defined by:

$$P = \left(\frac{d}{D}\right)^m \quad (1)$$

where  $P$  = weight fraction of particles less than diameter "d"  
 $D$  = maximum particle diameter  
 $m$  = a constant ranging from 0.33 to 0.5

A different approach, although still somewhat empirical, was that taken by Pivinski 6/, 7/. With this method, coarse-grained fillers are added to a slip to create a framework of coarse grains with its interstices filled with the finer material from the slip. The settling of large particles is avoided by increasing the volume per cent solids of the slip and filler to the point that the viscosity is sufficient to hold the coarse filler in suspension. The bulk density of a casting is given by:

$$\rho_{\text{cast}} = V_f \rho_T - 1 (1 - V_f) (\rho_o) \quad (2)$$

where  $V_f$ , the volume fraction filler in the casting, is given by:

$$V_f = \frac{W_f \rho_o}{\rho_T} \quad (3)$$

and where

$W_f$  = weight fraction filler  
 $\rho_o$  = bulk density of castings with no filler  
 $\rho_T$  = specific gravity of the solid phase

This relationship is said to hold for values of  $V_f$  up to 60-65 per cent, using fused silica. Above this range, there is insufficient slip to fill the voids in the filler packing and density begins to drop. As an example, a slip containing the maximum volume filler is said to have a specific gravity of 2.05 gm/cm<sup>3</sup>, a moisture content of up to 7 per cent, and a volume fraction solids of up to 87 per cent. Castings from this slip have minimum porosities of approximately 6.5 per cent, a value normally approached in well-sintered slip-cast fused silica. In actuality, this amounts to aggregate casting and requires vibration to fill the mold.

A final approach, on more of an analytical basis, is that of Lewis and Goldman 8/. In brief, their arguments are as follows. Most simple particle size distributions, whether casting slips, or screened powders, tend to follow a log normal size distribution. That is, the particle sizes are distributed normally with respect to the logarithm of particle diameter. When such a cumulative size distribution is plotted with the cumulative percentage on a probability scale, it follows a straight line. Analytically the line is defined by a minimum of two parameters, a point and a slope. In statistical terms, the point represents the mean diameter and the slope is equal to the inverse of the variance of the distribution. The broader the range of particle sizes, the less the slope of the straight line and the greater the variance of the distribution. They state that in general the packing efficiency of a particulate system increases with increasing variance (i.e., broader particle size distribution). Specifically, when blending two distributions, a higher packing efficiency will accompany an increase in the coefficient of variation of the system. The coefficient of variation is defined as the ratio of the variance to the log of the median particle diameter. A long series of analytical expressions for calculating the statistical properties of size distributions and of binary blends are given.

With all of these ideas in mind, the actual experimental program was begun.

## 2. Fused Silica Slip Characterization

A batch of high purity fused silica slip was purchased from Thermo Materials Corporation. Characterization data on the slip is shown in Table II and includes mean particle diameter (by sedimentation as in ASTM-D422), pH, and Brookfield viscosity.

A vendor-supplied chemical analysis of the slip is shown in Table III. The silica content is by difference. The alkali metals are determined by flame photometry, and the remaining oxides by quantitative emission spectroscopy.

These values and the particle size data meet the requirements of the current Georgia Tech specification for high purity fused silica slip suitable for radome manufacture.

Experience has shown that a bulk density of  $1.96 \text{ gm/cm}^3$  is a satisfactory density for radome and electromagnetic window requirements. Test bars, 3/4-inch diameter by 6-inch length, required 5-1/2 hours sintering at  $2210^\circ \text{ F}$  to reach this density. Physical, mechanical and electrical test data on samples sintered under these conditions are shown in Table IV.

### 3. Composite Development

#### a. Silicon Carbide Composites

A series of five SiC powders were obtained. Measured particle size distributions for the powders are shown in Figure 2. The mean particle diameters range from 3.5 to 13 micrometers.

Preliminary work on fused silica/SiC composites had been performed under a prior program 3/. Samples were sintered 16 hours in argon at  $2200^\circ \text{ F}$  with no attempt to optimize sintering for each composition. Some of the resulting data is shown in Table V. These results indicated that while a coarse SiC powder lowered the density of the sintered samples less, a powder with a mean particle size nearly the same as the fused silica slip produced the highest strengths. This suggested that the addition of comparatively coarse particles to the slip disturbed the packing efficiency less than did additions of fine powders, but that the greater surface area of fine powders might aid in sintering and strength development.

TABLE II  
 CHARACTERIZATION DATA OF THERMO MATERIALS FUSED SILICA SLIP  
 050972-2

Particle Size Distribution	Figure 1
Median Particle Size	7.3 $\mu\text{m}$
Per Cent Solids in Slip	82.76
Viscosity @ RPM	<u>Centipoise</u>
6	150
12	135
30	120
60	128
pH	4.6

TABLE III  
 CHEMICAL ANALYSIS OF THERMO MATERIALS SLIP 050972-2

<u>Oxide or Metal</u>	<u>Weight Per Cent</u>
$\text{Al}_2\text{O}_3$	0.310
$\text{TiO}_2$	0.003
$\text{Fe}_2\text{O}_3$	0.002
MgO	0.007
CaO	0.002
Na	<0.001
K	<0.001
Li	<0.001
$\text{SiO}_2$	99.670

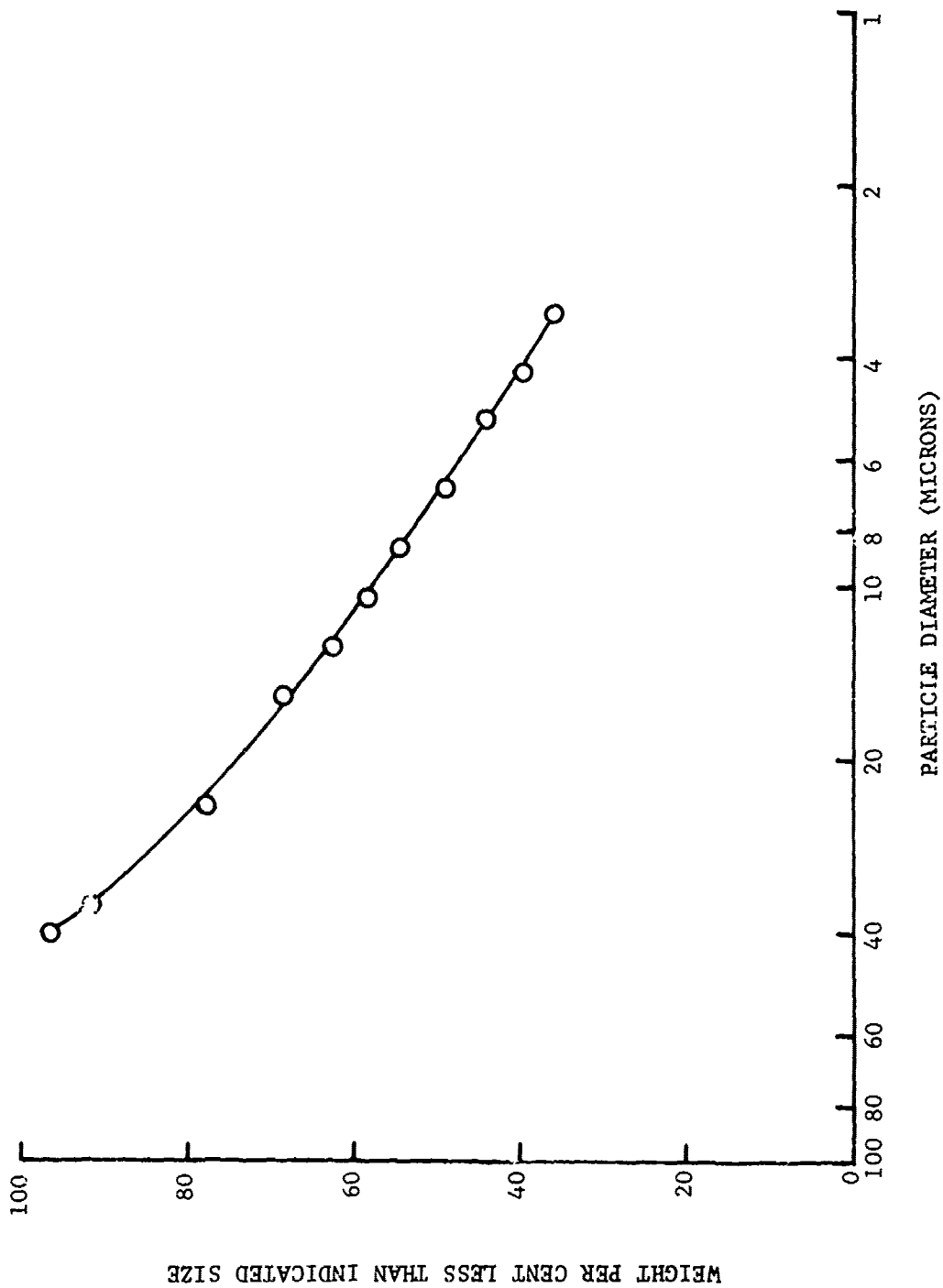


Figure 1. Particle Size Distribution-High Purity Fused Silica Slip.

TABLE IV

CHARACTERIZATION DATA ON 3/4-INCH DIAMETER CYLINDRICAL TEST  
SPECIMENS SLIP-CAST FROM THERMO MATERIALS SLIP 050972-2  
AND SINTERED 5-1/2 HOURS AT 2210° F

Per Cent Water Absorption	5.18 ± 0.05
Per Cent Porosity	10.14 ± 0.09
Bulk Density	1.960 ± 0.002 gm/cc
Apparent Specific Gravity	2.181 ± 0.002 gm/cc
Flexural Strength	5136 ± 526 psi
Modulus of Elasticity	5.82 ± 0.12 × 10 <sup>6</sup> psi
Thermal Expansion	0.45 × 10 <sup>-6</sup> /°C

## Dielectric Properties\*

<u>Temperature</u>		<u>Dielectric Constant</u>	<u>Loss Tangent</u>
(°C)	(°F)		
24	75	3.36	0.0008
260	500	3.39	0.0009
566	1051	3.45	0.0015
816	1500	3.49	0.0025
982	1800	3.53	0.0030

\*Actual density of dielectric test specimens was 1.947 gm/cc.

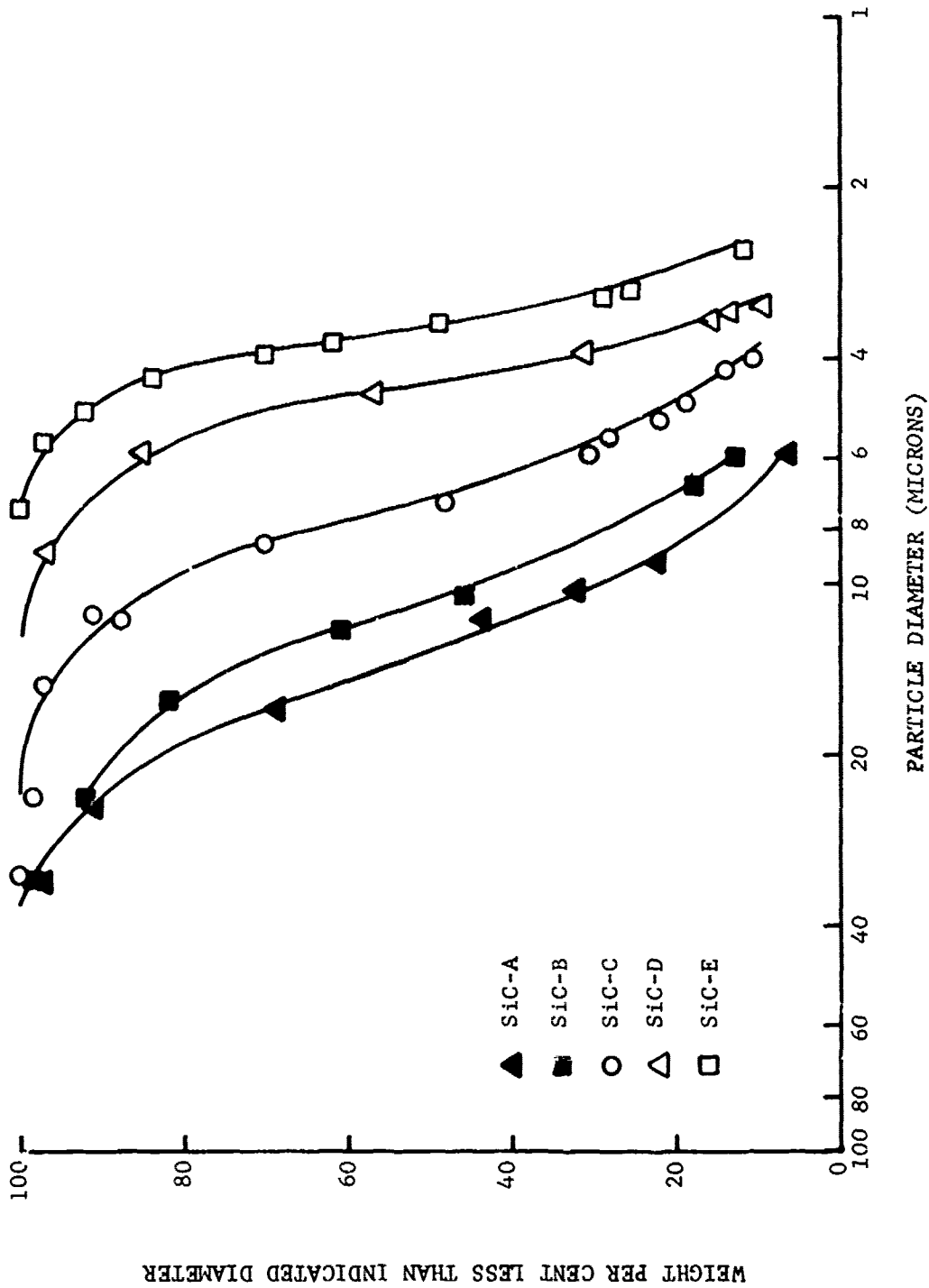


Figure 2. Particle Size Distribution - Silicon Carbide Powders.

TABLE V  
 MEAN VALUES OF PROPERTIES OF SiO<sub>2</sub>-SiC COMPOSITES

Sample	Additive Volume (%)	Specific Gravity	Bulk Density	Porosity (%)	Dynamic Elastic Modulus (psi x 10 <sup>6</sup> )	Modulus of Rupture (psi)
SiO <sub>2</sub>	0	2.21	2.04	8.63	6.76	6369
SiC-31μ	5	2.26	2.05	9.37	5.39	5533
SiC-31μ	10	2.32	2.16	6.98	5.38	5945
SiC-31μ	20	2.41	2.19	8.94	4.25	5074
SiC-7μ	5	2.28	2.07	9.00	6.77	8159
SiC-7μ	10	2.34	1.93	17.54	3.24	2726
SiC-7μ	20	2.43	1.84	24.34	3.05	2832

As a first attempt, an additive was selected to match the particle size of the fused silica slip as closely as possible. Since powder "C" had approximately the same mean particle diameter, it was a logical candidate. However, since it was essentially a monofraction, the slope of the distribution was much steeper. To broaden the distribution a slip was prepared from equal volumes of powders A, C and E.

NOTE: Since sedimentation particle size distribution techniques are not applicable to mixtures of particles of different specific gravity, a simple scheme was used to predict particle size distributions. The powder distributions and the slip particle size distribution were plotted on log-probability paper and fitted with best fit straight lines. These lines were used to calculate fitted values for the cumulative percentage at various particle diameters. The percentage at any diameter on a composite slip was calculated by summing the appropriately weighted percentages for each component at that diameter. This technique is used throughout this report.

The equal blend of powders A, C and E was added to the slip in volumes of 5, 10 and 15 per cent. For further comparison, 10 volume per cent additives of powders A, C and E were made individually. Fifteen test samples, 2-1/2 inches long by 3/4-inch diameter were cast from each composition. After casting in plaster molds, the samples were removed, dried at 350° F and trimmed with a silicon carbide grinding wheel so that their ends were parallel and perpendicular to the longitudinal axis of the bar. Bulk density, and dynamic Young's modulus for each sample were measured. Then three samples from each composition were sintered at 2300° F for various times. Sintered bulk density, sintering shrinkage, and change in both bulk density and per cent theoretical density were calculated for each

sample. Figure 3 shows per cent theoretical density as a function of sintering time for the three compositions and the fused silica controls.

Each sintered sample was then cut into four discs, 3/4-inch diameter by 3/8-inch long. These discs were stood on edge and broken in diametral compression to determine tensile strength. The average tensile strengths for each material as a function of sintering time are shown in Figure 4.

At this point samples were prepared from slips containing 10 v/o of the two binary 2:1 blends of each of the three powders A, C and E. Test procedures were as before. Data for all thirteen compositions are tabulated in Appendix I.

As a preliminary step in data analysis, dry per cent theoretical density (packing efficiency), per cent weight gain at 8 hours sintering time, maximum per cent theoretical density, per cent change in bulk density, and maximum tensile strength were all plotted on ternary diagrams as functions of additive composition, Figure 5. From these plots, several trends were noted. Dry density tended to decrease with finer powder additions. In addition, the oxidation weight gain, the sintering rate, and the maximum tensile strength all increased with finer powder additions.

In order to assess analytically the effects of compositional variables, and size distribution parameters on the packing efficiency of the slip, several steps were taken. First, particle size distributions were calculated and log-probability plots were made for each of the twelve composite slips and the fused silica slip. Best fit straight lines and correlation coefficients were calculated for each distribution over the range 1 to 30 micrometers as shown in Figure 6, which shows the particle size distribution of a slip containing 10 per cent powder E.

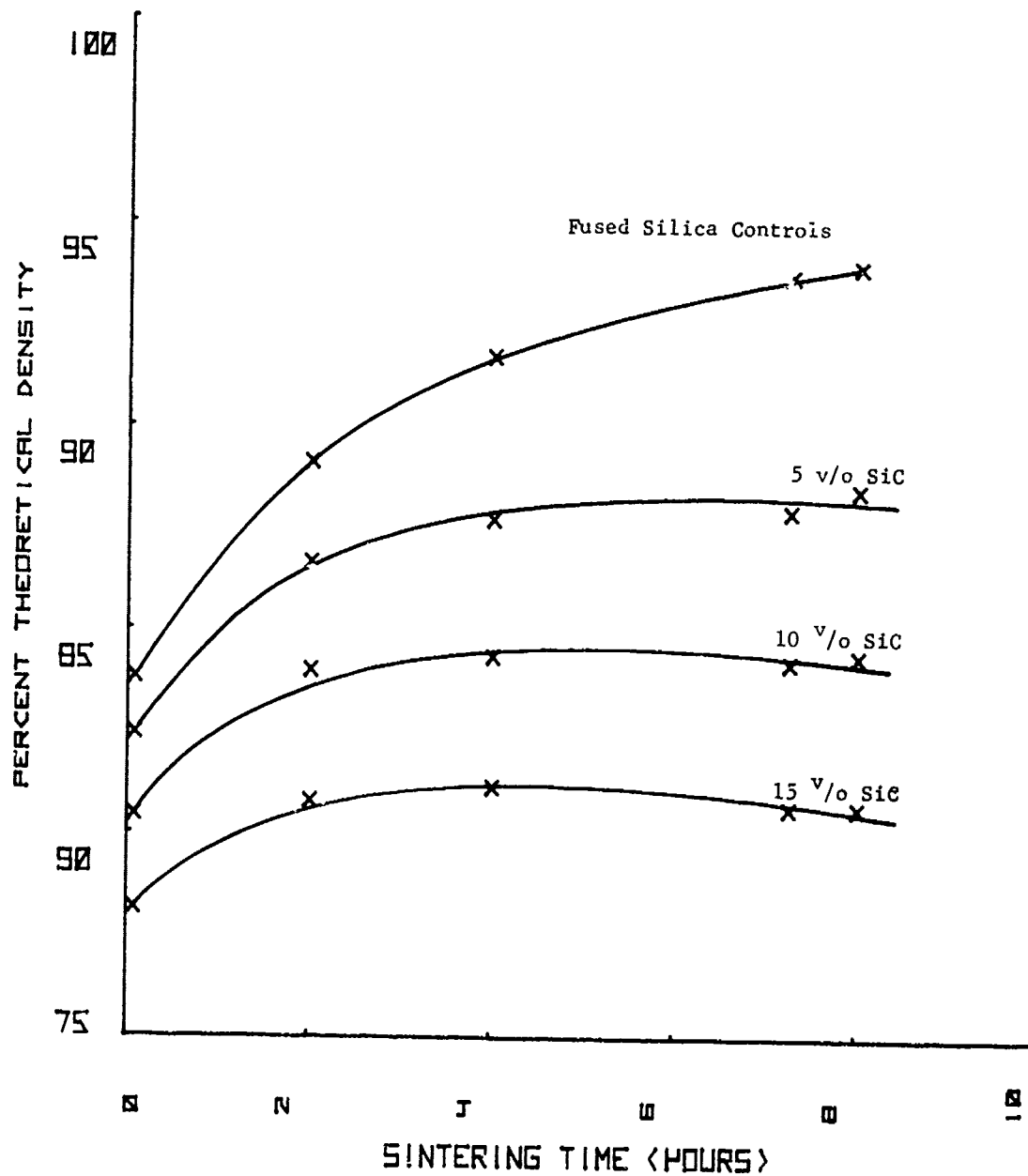


Figure 3. Per Cent Theoretical Density Versus Sintering Time at 2300° F for Slip-Cast Fused Silica with 0 to 15 Per Cent Additions of Equal Parts Silicon Carbide A, C, and E.

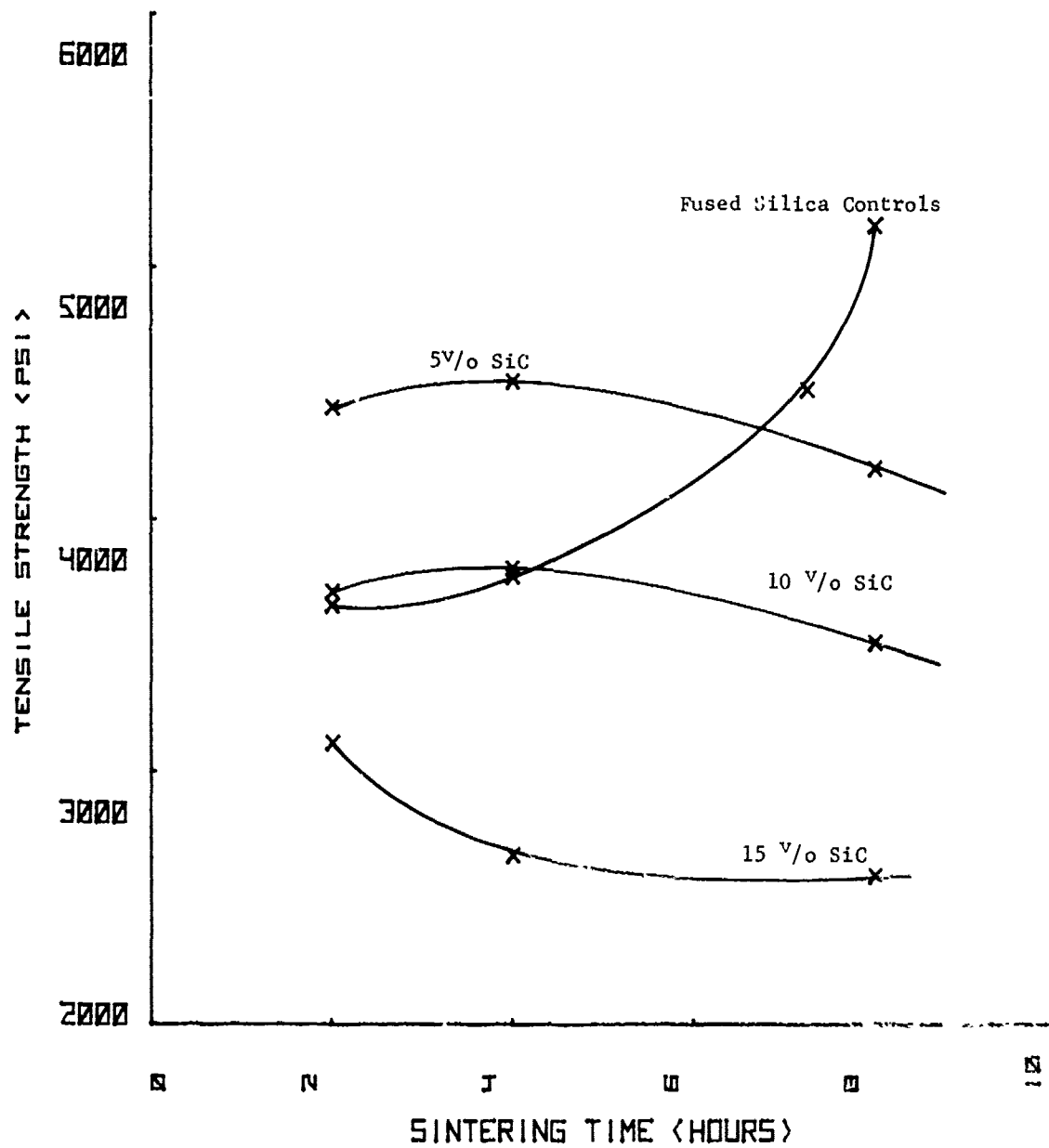


Figure 4. Tensile Strength Versus Sintering Time at 2300° F for Slip-Cast Fused Silica with 0 to 15 Per Cent Additions of Equal Parts Silicon Carbide A, C, and E.

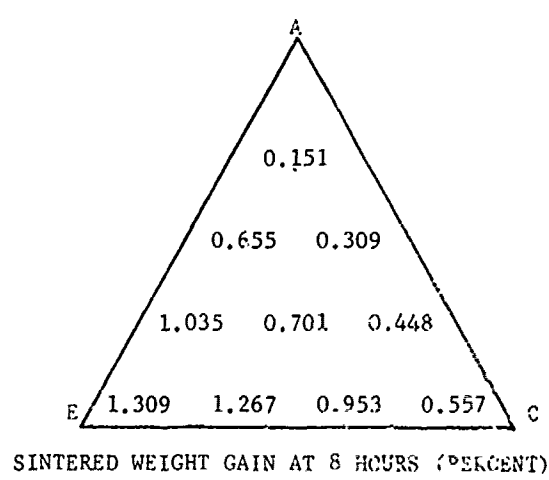
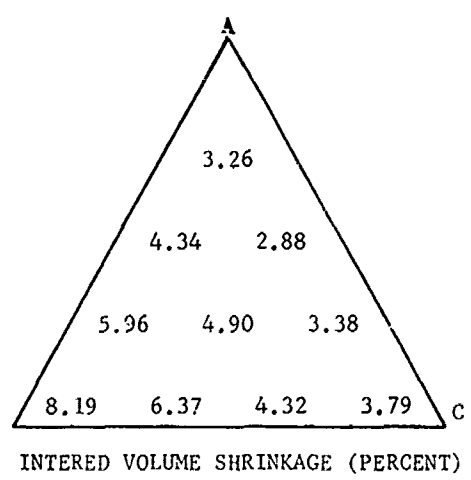
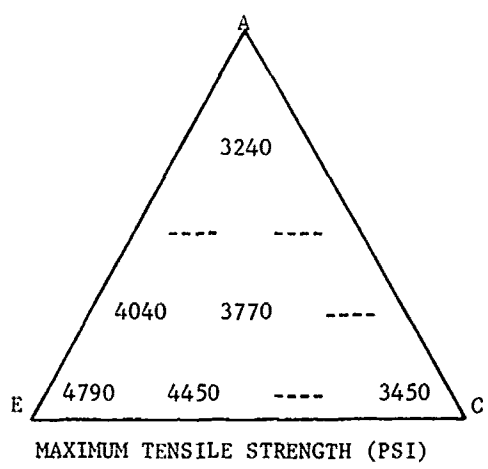
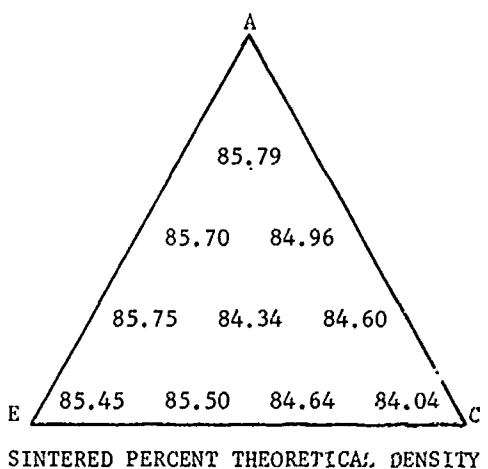
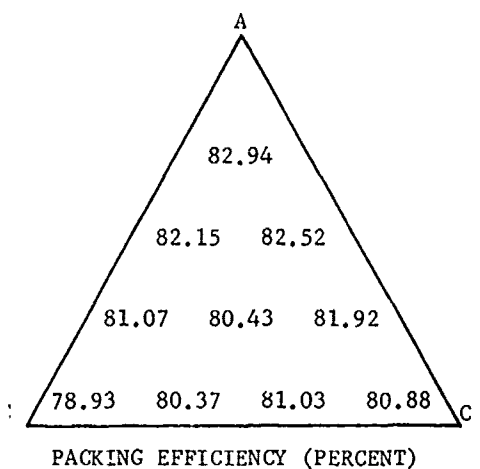


Figure 5. Sintering Data Versus Composition for 10 per cent SiC/SiO<sub>2</sub> Composites

The numerical value for the slope (units of probits/μm particle diameter) was assumed to be proportional to the reciprocal of the variance. From this, a coefficient of variance was calculated as the product of the slope and the natural log of the mean particle diameter, as in 8/. To assess the effect of surface area on packing efficiency, a figure of merit, referred to as "fineness," was defined as being proportional to the reciprocal of the mean particle diameter squared. The values were normalized to set the maximum value (for powder E) equal to ten. The final data used in the analysis is shown in Table VI.

A multiple linear correlation analysis was performed on the data with the per cent theoretical density as the dependent variable. The matrix of correlation coefficients is shown in Table VII.

The results of this analysis showed that the only significant correlation was between fineness and the per cent theoretical density of the casting, suggesting that an excess of fineness in the particle size distribution was lowering the packing efficiency. The remaining correlation greater than 0.5 is a forced correlation between slope and coefficient of variation and is not significant.

Since Lewis and Goldman 8/ had found a parabolic relationship between coefficient of variance and packing efficiency, the data were plotted as shown in Figure 7. The data points fall on two lines. The first, with positive slope, agrees with Lewis and Goldman 8/. This line passes through the unmodified slip and the 5, 10 and 15 v/o additions of the equal blend. The remaining points lie on a straight line with negative slope and are defined by all of the compositions containing 10 v/o SiC. The data suggest that the Lewis and Goldman relationship holds true for simple binary blends (i.e., fused silica slip and a single SiC composition), but not for a more complex situation

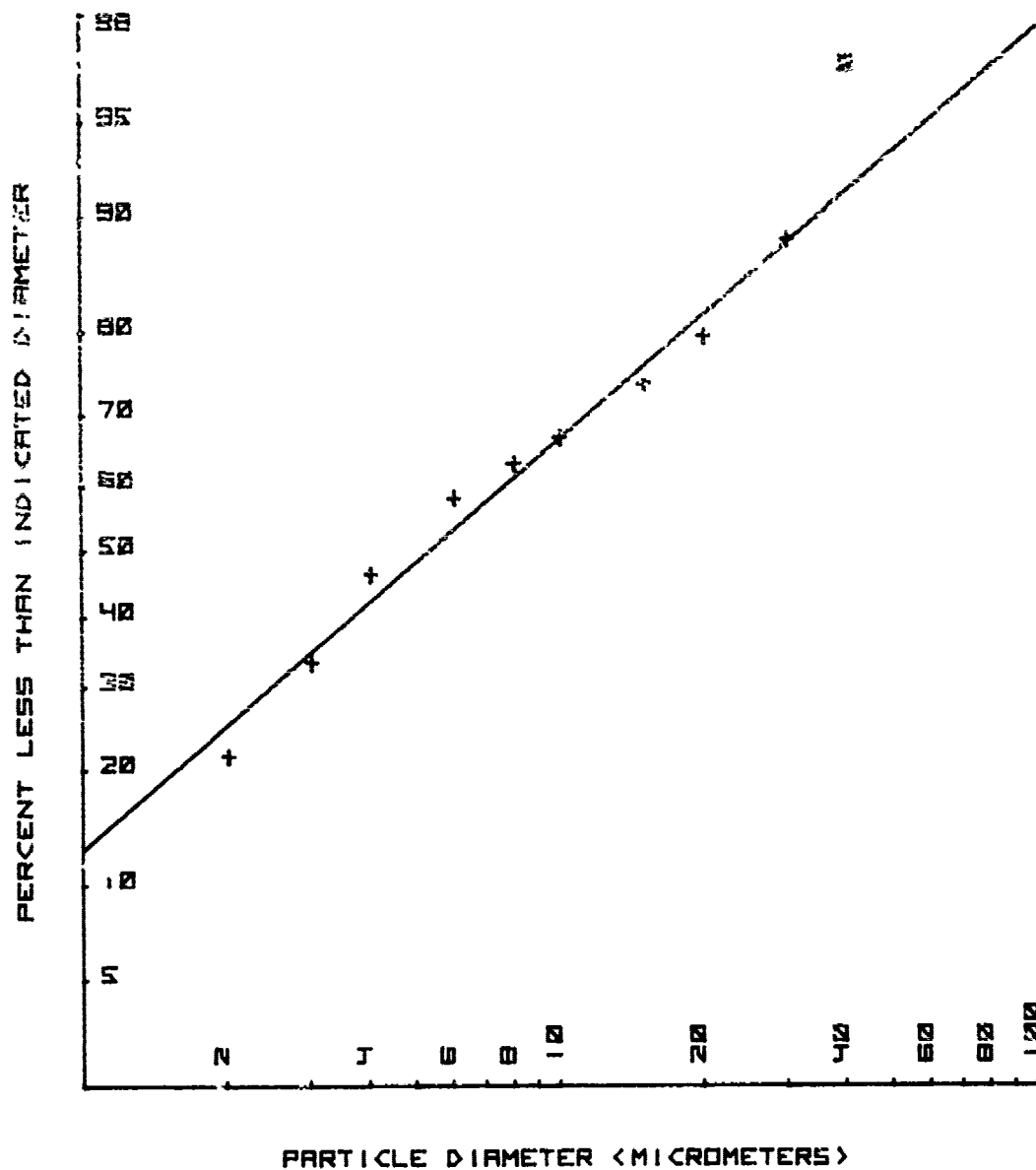


Figure 6. Calculated Particle Size Distribution and Best Fit Line for Composite Slip with 10 Per Cent Silicon Carbide Powder E.

with four components. The data further suggest that the line formed by the 10 v/o SiC composition represents a contour line of constant additive proportion and that parallel lines probably exist for the same range of compositions at the 5 and 15 v/o levels.

A second multiple linear correlation analysis was performed on the data in Table VI. This time the values for the fused silica slip and the 5 and 15 v/o SiC addition were deleted. The revised correlation matrix is shown in Table VIII. This time a strong positive correlation is observed for fineness and coefficient of variation, and a strong negative correlation for coefficient of variance and the packing efficiency. The former is probably forced to some extent by the method of calculating the coefficient of variation and the fineness from the mean particle diameter, but the latter correlation is a true correlation.

As a final attempt at analysis, the best and worst cases were plotted along with the Andreasen relationship, Figure 8. The fused silica slip was used as a best case, and the 15 v/o equal blend as the worst case. The Andreasen relationship is simply not selective enough to be of application here.

A similar analysis was performed to determine the effect of various process parameters on tensile strength and to determine some of the interrelationships between measured properties of the sintered composites. For the purpose of analysis, the maximum tensile strength was taken as the dependent variable, and the per cent theoretical density (packing efficiency) of the dried castings and the fineness of the additive SiC were taken as independent variables, although they have been previously shown to be interrelated. The maximum per cent theoretical density, the per cent volume shrinkage, and the per cent weight change on sintering were also considered as independent variables, when in reality they were dependent variables. The data

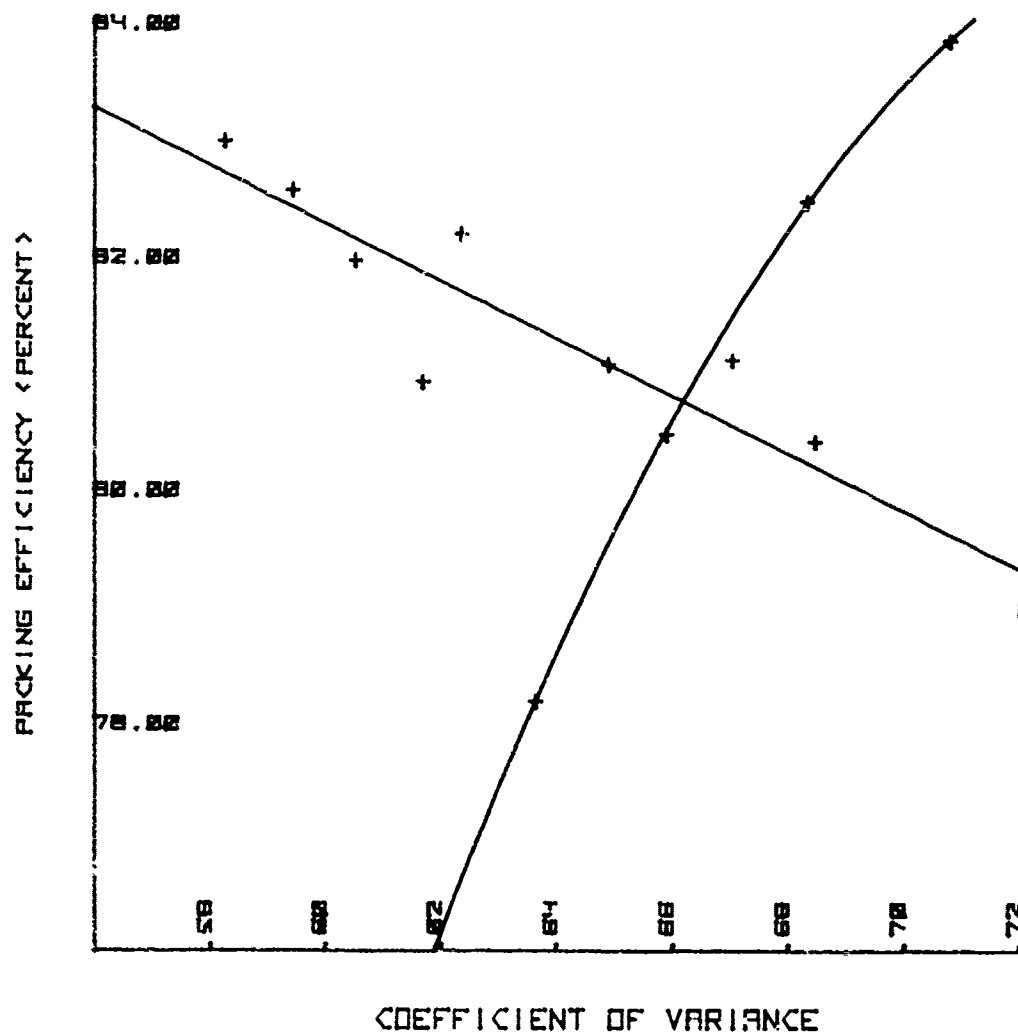


Figure 7. Packing Efficiency Versus Coefficient of Variance for SiC/SiO<sub>2</sub> Composites.

TABLE VI  
DATA MATRIX FOR PACKING EFFICIENCY CORRELATION ANALYSIS

ADDITIVE		Particle Size Distribution						
A	C	Weight Ratio		Slope (1/Variance)	Correlation Coefficient (Goodness of Fit)	Fineness (1/d <sup>2</sup> )	Coefficient of Variance	Packing Efficiency (%)
		E	Volume Per Cent					
0	0	0	0	0.58219	0.98211	0	0.7079	83.81
1	1	1	5	0.62425	0.98799	2.011	0.6832	82.43
1	1	1	10	0.66668	0.99196	4.021	0.6590	80.43
1	1	1	15	0.71010	0.99501	6.032	0.6364	78.14
3	0	0	10	0.70508	0.96171	0.767	0.5825	82.94
0	3	0	10	0.74749	0.99421	1.296	0.6170	80.88
0	0	3	10	0.68181	0.98184	10.000	0.7255	78.93
1	2	0	10	0.73282	0.98888	3.359	0.6053	81.92
2	1	0	10	0.71837	0.97817	2.830	0.5943	82.52
1	0	2	10	0.68845	0.99300	6.922	0.6703	81.07
2	0	1	10	0.69676	0.98519	3.844	0.6236	82.15
0	1	2	10	0.70324	0.99515	7.099	0.6846	80.37
0	2	1	10	0.72498	0.99880	4.197	0.6940	81.03

TABLE VII  
CORRELATION CO-EFFICIENT MATRIX  
PACKING EFFICIENCY STUDY

	<u>Slope</u>	<u>Fineness</u>	<u>Coefficient of Variance</u>	<u>Packing Efficiency</u>
Correlation Co-efficient	0.17048	0.35575	0.30992	-0.51310
Slope		0.21311	-0.65442	-0.37313
Fineness			0.46203	-0.78269
Coefficient of Variance				-0.25193

TABLE VIII  
REVISED CORRELATION CO-EFFICIENT MATRIX  
(10% Composites Only)

	<u>Slope</u>	<u>Fineness</u>	<u>Coefficient of Variance</u>	<u>Packing Efficiency</u>
Correlation Co-efficient	0.12675	0.31171	0.44672	-0.51323
Slope		-0.54789	-0.55808	-0.37180
Fineness			-0.93387	-0.78031
Co-efficient of Variance				-0.92721

matrix is shown in Table IX. Values of per cent theoretical density and per cent change in theoretical density correspond to the sintering times for the indicated maximum tensile strength.

The matrix of multiple linear correlation coefficients is shown in Table X. From this it can be seen that the packing efficiency (dry per cent theoretical density) decreases with increasing fineness of the SiC additive. However, the sintering rate, as indicated by the per cent volume shrinkage, increases with increasing fineness, resulting in increased tensile strength. In fact, tensile strength tends to vary inversely with the packing efficiency of the slip, the reverse of the expected trend. The major result of the analysis is that tensile strength increases with increasing fineness or surface area of the additive. The mechanism of such an increase is unknown, but it is suspected that the silicon oxide film produced on the surface of the SiC particles during sintering makes the particles more compatible with the silica particles. Most of the remaining correlations are forced correlations of dependent variables.

It was suspected that the amount of additive as well as its particle size distribution also had a definite effect on the tensile strength of composites. The data for the 5, 10, and 15 per cent additions of the equal blend of powders A, C, and E, as shown in Table XI, show that as the amount of additive increases, the packing efficiency, the sintering rate (per cent change in density) and the tensile strength decrease. In fact, the correlations are nearly linear as shown in Table XII. As with the packing efficiency study, the response surface for tensile strength as a function of additive volume and composition is complex, and many more compositions would have to be examined to define it properly.

TABLE IX

DATA MATRIX FOR EFFECTS OF SLIP PROPERTIES ON  
SINTERING PROPERTIES AND TENSILE STRENGTH

Packing Efficiency	Fineness	Sintered Per Cent Theoretical Density	Per Cent Volume Shrinkage	Per Cent Weight Gain	Tensile Strength
82.94	.767	85.79	3.26	0.151	3244
81.07	6.922	85.75	5.96	1.035	4035
80.43	4.021	84.34	4.90	0.701	3767
78.93	10.00	85.45	8.19	1.309	4785
80.37	7.099	85.50	6.37	1.267	4445
80.88	1.296	84.04	3.79	0.557	3450

TABLE X

CORRELATION COEFFICIENT MATRIX FOR EFFECTS OF SLIP  
PROPERTIES ON SINTERING PROPERTIES AND TENSILE STRENGTH

	Fineness	Sintered Per Cent Theoretical Density	Per Cent Volume Shrinkage	Per Cent Weight Gain	Tensile Strength
Packing Efficiency	-.79363	.20890	-.84721	-.74262	-.84434
Fineness	----	.40663	.39056	.86813	.97486
Sintered Per Cent Theoretical Density	----	----	.33978	.20236	.32581
Per Cent Vol. Shrinkage	----	----	----	.83876	.98619
Per Cent Weight Gain	----	----	----	----	.88015

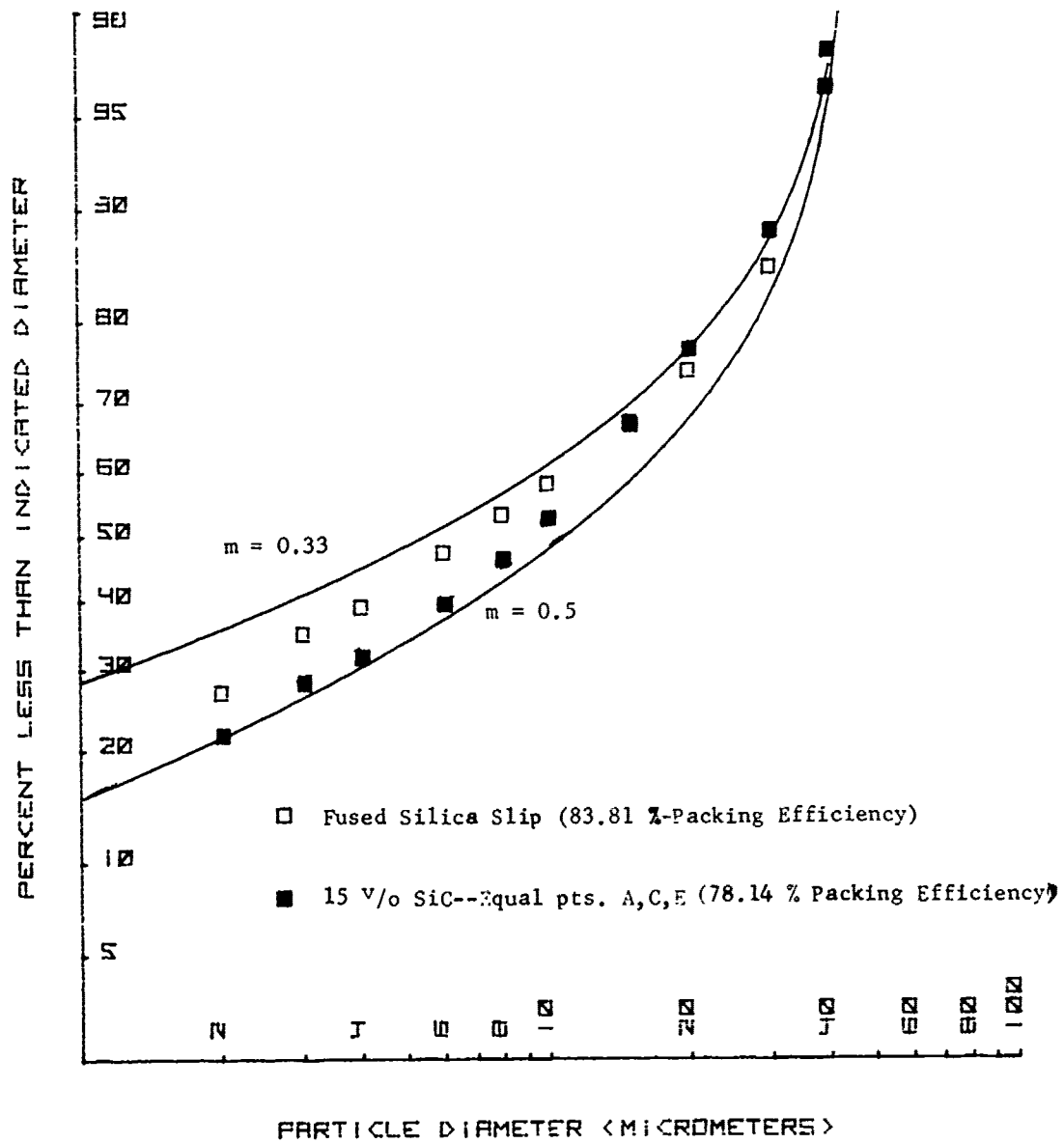


Figure 8. Particle Size Distributions of Maximum and Minimum Packing Efficiency, and Range of Size Distributions for Maximum Packing From Andreasen Relationship.

TABLE XI  
EFFECT OF ADDITIVE  
VOLUME ON TENSILE STRENGTH

<u>Volume Per Cent Additive</u> (%)	<u>Packing Efficiency</u> (w/o)	<u>Per Cent Change in Bulk Density</u> (%)	<u>Tensile Strength</u> (psi)
0	83.81	11.95	5160
5	82.43	6.33	4540
10	80.43	4.90	3770
15	78.14	3.34	3100

TABLE XII  
CORRELATION COEFFICIENT MATRIX -  
ADDITIVE VOLUME EFFECTS

	<u>Packing Efficiency</u>	<u>Per Cent Change in Bulk Density</u>	<u>Tensile Strength</u>
Volume Per Cent Additive	-0.99417	-0.93822	-0.99922
Packing Efficiency		-0.89694	0.99513
Per Cent Volume Shrinkage			0.92713

It might have been possible to achieve higher densities and strengths by resorting to the aggregate casting technique 6/, 7/ and loading the slip with relatively coarse grain. However, the presence of large grains in a slip-cast fused silica material create complicated machining since they are prone to pull out in grinding. In addition, size segregation caused by differential sedimentation is difficult to control unless paste-like compositions are used. For these reasons, this type of approach was not considered.

In summary, the SiC composite study showed that the particle size of the addition was the controlling factor in obtaining high strength materials. After reviewing both data from the current program and from past programs, a composite containing 10 per cent SiC powder "E", sintered four hours at 2300° F, was established as the optimum material.

#### b. Silicon Nitride Composites

In view of what had been learned on SiC composite development, a single silicon nitride powder was purchased. The material was reported as 95 per cent purity with the major impurity free silicon. X-ray diffraction analysis confirmed this and showed that the powder was predominantly  $\epsilon$ - $\text{Si}_3\text{N}_4$ , the high temperature phase. The particle size distribution curve for the material is shown in Figure 9. This particular grade of powder was chosen for its particle size range (1-5 micrometers by manufacturer's specification). However, the particle size analysis indicated a mean diameter of 10 micrometers. The distribution was not log normal and as such may have been a blended powder.

Slips containing 5, 10 and 15 v/o  $\text{Si}_3\text{N}_4$  were prepared and samples were cast and sintered as in the SiC study. A preliminary sintering

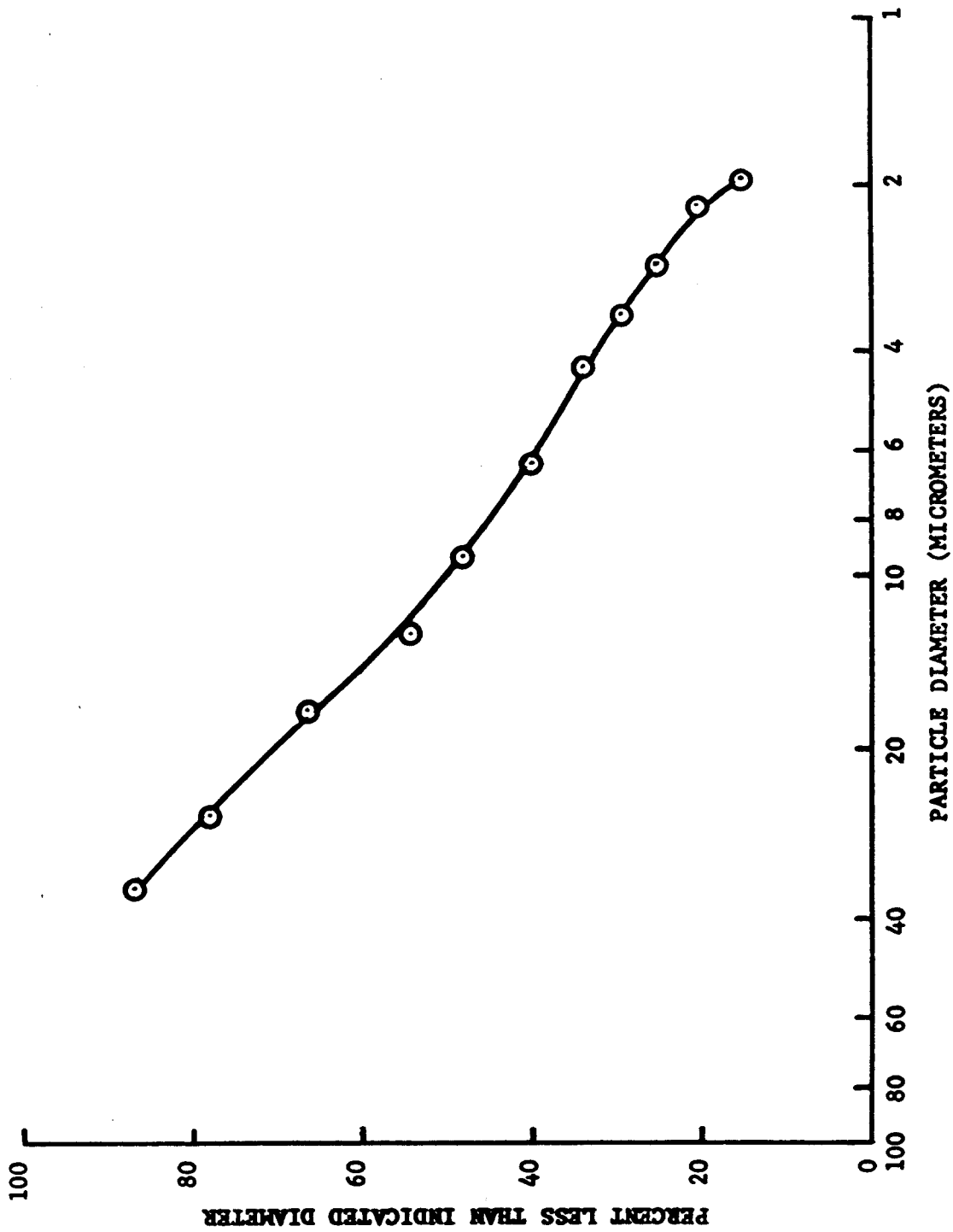


Figure 9. Particle Size Distribution for Silicon Nitride Powder.

indicated that even at the 2300° F sintering temperature, the oxidation of the nitride powders was too rapid to permit adequate sintering. The remaining samples were sintered in a nitrogen atmosphere. The packing efficiencies of the samples were 80.2, 78.5 and 74.5 per cent, at the 5, 10 and 15 v/o levels, respectively. These values are consistently about 4 per cent lower than the comparable values for the SiC composites, indicating that differences in particle shape or, more probably, in the additive size distribution are significant. For further comparison with the SiC composites, Table XIII shows data corresponding to that in Table XI.

TABLE XIII  
SINTERING DATA FOR  $\text{Si}_3\text{N}_4$  COMPOSITES

<u>Volume Per Cent Additive</u> (v/o)	<u>Packing Efficiency</u> (%)	<u>Sintering Volume Shrinkage</u> (%)	<u>Maximum Tensile Strength</u> (psi)
0	83.81	11.95	5160
5	80.24	8.26	4920
10	78.54	8.33	4540
15	74.45	8.31	2950

The greatest apparent difference in the two materials is that the  $\text{Si}_3\text{N}_4$  sintering rate is not volume dependent. Although strengths decreased with increasing additive content, the sintering rate remained nearly the same. In addition, at both the 5 and 10 v/o levels, the  $\text{Si}_3\text{N}_4$  composites were stronger (tensile strength) than SiC composites, indicating more and stronger interparticle bonding.

Of the materials studies, the 10 v/o  $\text{Si}_3\text{N}_4$  composite sintered 6 hours at 2300° F in nitrogen was selected as having optimal mechanical and physical properties.

### c. Boron Nitride Composites

Previous work at Georgia Tech 9/ had encountered difficulty in preparing BN/ $\text{SiO}_2$  composites. The castings were soft and fragile, while sintering usually resulted in rapid devitrification. Possible thin layers of  $\text{B}_2\text{O}_3$  on the surface of the BN particles were suggested as the major source of difficulty.

To eliminate the possibility of  $\text{B}_2\text{O}_3$  formation from reaction with water, an anhydrous slip was prepared. Since electrophoretic deposition requires the same suspending properties as a casting slip, and since acetone has been reported as a successful vehicle for electrophoretic deposition of silica 10/, acetone was selected as the liquid portion of the slip. A gallon of the high purity slip was spray dried, and the resulting powder was dried at 350° F. Ten volume per cent BN slips were prepared using both acetone and water as suspending agents. Both slips were highly dilatant and required dilution to 50 per cent solids before a usable slip could be obtained. As with the SiC and  $\text{Si}_3\text{N}_4$  composites, short test bars were cast. In both cases, the castings adhered to the mold walls and the castings could not be removed intact. Since the mold release agents commonly used, (i.e., graphite and ammonium alginate) both required oxidation for complete removal from the casting, and since the cast parts were so fragile, work with boron nitride was suspended.

## 4. Composite Characterization

### a. Physical and Mechanical Testing

Samples of the successful composites, SiC/ $\text{SiO}_2$  and

$\text{Si}_3\text{N}_4/\text{SiO}_2$ , were prepared for physical, mechanical and electrical testing. The samples were cylindrical bars, 3/4-inch diameter by 6 inches long. The  $\text{SiC}/\text{SiO}_2$  composites were sintered in air for 4 hours at 2300° F, while the  $\text{Si}_3\text{N}_4/\text{SiO}_2$  composites were sintered in nitrogen for 6 hours at 2300° F. After firing, samples were trimmed to a five-inch length, and porosity, bulk density, and specific gravity were determined with the boiling water technique. Then dynamic Young's modulus was measured with a sonic flexural resonance method. The samples were then broken in 4-point quarter point loading to determine modulus of rupture. Results from all of these tests, along with the comparable data from the fused silica slip characterization, are presented in Table XII.

b. Electrical Testing

Dielectric constant and loss tangent were measured at temperatures from ambient to 1800° F. The results of these tests are shown in Table XIII.

c. Ablation Resistance Testing

A number of 2-inch diameter, 1/2-inch thick test specimens were prepared for ablation. The samples were positioned six inches from the nozzle exit plane of a small oxygen-hydrogen rocket motor. At this point, the heat flux has been measured at 1500 Btu/ft<sup>2</sup>-sec., and the stagnation pressure at 2.4 psi, 11/. Exposure times were 30 seconds for all materials. Front and back surface temperatures were monitored with an infrared pyrometer and chromel/alumel thermocouples, respectively.

The rocket motor performance was not consistent and resulted in widespread variation between individual samples. In general, results may be summarized as follows:

- (1) Slip-Cast Fused Silica: Measured front surface temperature ranged from 3100 to 3360° F. All

TABLE XIV

## CHARACTERIZATION DATA ON FUSED SILICA COMPOSITES

	<u>Slip-Cast Fused Silica</u>	<u>Slip-Cast Fused Silica w/ 10% SiC</u>	<u>Slip-Cast Fused Silica w/ 10% Si<sub>3</sub>N<sub>4</sub></u>
Per Cent Porosity	10.14±0.09	8.69±1.15	12.73±.44
Bulk Density	1.960±0.002 gm/cc	2.020±0.032 gm/cc	1.969±.006 gm/cc
Apparent Specific Gravity	2.181±0.002 gm/cc	2.213±0.026 gm/cc	2.257±.015 gm/cc
Flexural Strength	5140±530 psi	3480±810 psi	1660±370 psi
Tensile Strength	3650±1130 psi*	4450±330 psi	4540±510 psi
Modulus of Elasticity	5.82±0.12x10 <sup>6</sup> psi	7.48±0.18x10 <sup>6</sup> psi	6.27±.15x10 <sup>6</sup> psi

\* Values for fused silica samples at density. Maximum tensile strength 5160 ± 1060 psi @ 2.085 gm/cc.

TABLE XV

DIELECTRIC CONSTANT AND LOSS TANGENT FOR  
SiC/SiO<sub>2</sub> AND Si<sub>3</sub>N<sub>4</sub>/SiO<sub>2</sub> COMPOSITES

<u>Composition</u>	<u>Temperature (°F)</u>	<u>Dielectric Constant</u>	<u>Loss Tangent</u>
10% SiC	RT	4.16	0.03
	500	4.23	0.03
	1075	4.37	0.19
	1460	4.42	0.065
10% Si <sub>3</sub> N <sub>4</sub>	RT	3.45	0.003
	500	3.48	0.0008
	1075	3.58	0.008
	1460	3.62	0.009

samples developed a vitrified surface layer. Both its thickness and the degree of ablation varied directly with the observed surface temperature. Extensive rippling of the surface was observed only on samples at the upper end of the temperature range. No appreciable volume of material was removed from any of the samples. Only slight shrinkage from increased densification was observed.

- (2) SiC/SiO<sub>2</sub> Composites: Front surface temperature ranged from 3100 to 3460° F, indicating increased emittance. On the lower temperature samples only slight surface fusion was observed. On the higher temperature samples, a thin frothy melt layer was formed, but in no case was a deep translucent glazed layer formed, as in the slip-cast fused silica specimens.
- (3) Silicon Nitride: The Si<sub>3</sub>N<sub>4</sub>/SiO<sub>2</sub> test samples fell in the same front surface temperature range as the SiC/SiO<sub>2</sub> specimens; the glazed surface layer was slightly deeper than for SiC/SiO<sub>2</sub>, and the rippling of the surface was only slightly less than observed on the fused silica controls. As with the SiC/SiO<sub>2</sub> composites, ablation effects were limited to a thin surface layer and no thick glassy layer was formed as with the silica controls.

In summary, the SiC/SiO<sub>2</sub> composites were clearly superior. The Si<sub>3</sub>N<sub>4</sub>/SiO<sub>2</sub> composites were at worst comparable with slip-cast fused silica and at best only slightly inferior to the SiC/SiO<sub>2</sub> materials.

#### d. Rain Erosion Resistance Testing

A series of 2-inch diameter by 1/2-inch thick discs of the

two composites and slip-cast fused silica controls were tested for rain erosion resistance by impacting the sample with number nine lead shot at a velocity of approximately 1100 ft/sec. The angle of impact was increased gradually until a maximum angle of 90°, or normal impact, was reached. No significant differences in behavior of the sample were noted, particularly in the angle required to produce actual pitting, or material removal. If anything, the composite samples had a greater tendency to shatter at normal impact than did the silica controls. This failure was thought to be due to tensile failure at the back surface of the sample through bending, rather than from actual failure of the sample at the damage site on the front surface. In several instances, particularly with silicon nitride additives, the actual damage site was found to be smaller in area and depth than in the unmodified slip-cast fused silica. For the additive concentrations used and under these test conditions, no differences in impact behavior were noted for either of the composites or controls.

### C. Discussion

The extensive study of the SiC/SiO<sub>2</sub> composites demonstrated several items. First, present theories on particle packing are not adequate to describe the composites used on this program, and second, the controlling factor in tensile strength of the composite is the degree of sintering, which is controlled by the surface area of the additive, rather than by the packing efficiency of the casting. The latter is most probably due to the increased number of silica particle contacts in the slip with finer additives and to the increased reactivity of the higher surface area additive.

The flexural strengths of the SiC and Si<sub>3</sub>N<sub>4</sub> composites were lower than expected, especially in view of the relatively high tensile strength achieved. The most likely explanation for this behavior, as well as for the fact that tensile strength was not as highly dependent on sintering

time as flexural strength, is that the tensile test reflects the strength of the bulk material, while the flexural strength is affected greatly by the condition of the sample surface. In this case the surface of the samples would be expected to be in a damaged condition due to surface devitrification, resulting in low flexural strength values. In all probability, the tensile strength and elastic modulus are considered to be more indicative of the true strength of the material than is flexural strength. The flexural strength of the samples could probably have been improved by removal of the surface layer which normally contains the greater portion of the cristobalite in the sample.

The ablation resistance of the composite materials represents a slight improvement over that of normal slip-cast fused silica. The lack of densification and flow in the front surface layer seems to indicate an increased viscosity which, in turn, would result in less densification on fusion, and in lower creep rates, both of which are desirable improvements in cases where relatively long exposure to high temperature and high mechanical loads are encountered.

#### D. Conclusions

1. Silicon carbide and silicon nitride are effective in increasing the ablation resistance of slip-cast fused silica, with no adverse effects on rain erosion resistance and only minor losses in mechanical strength.
2. Boron nitride is not a satisfactory additive for use in slip-cast fused silica, although its use might still be possible with alternate fabrication techniques such as hot pressing.
3. In the composites studied, maximum tensile strengths were best realized through use of additives with high surface areas.

#### E. Recommendations

1. Studies should be made of elevated temperature creep and tensile properties of  $\text{SiC/SiO}_2$  and  $\text{Si}_3\text{N}_4/\text{SiO}_2$  composites since these materials show promise of being useful as structural materials.

2. Studies should be made to define the rain erosion resistance of the composites at elevated temperatures, since normal slip-cast fused silica relies on plastic flow to relieve impact loads.

3. Alternative methods of forming composites, such as aggregate casting, isostatic pressing, and hot pressing should be examined for usefulness in improving mechanical properties of the composites.

This page intentionally left blank.

SECTION II  
ISOSTATIC PRESSING OF FUSED SILICA

A. Introduction

1. Program and Objectives

The objective of work carried out under Contract No. DAAH01-72-C-0400 was to develop a method other than slip casting for the fabrication of rebonded fused silica radomes. Slip casting has been found to be relatively slow and expensive when a high production rate is necessary. Isostatic pressing is a forming process used to fabricate alumina radomes, and offers attractive features which include: a) lower moisture contents, thus shorter drying time and b) the potential for rapid forming cycles. Isostatic pressing has not been emphasized in the past because slip casting procedures are satisfactory for fabricating trial shapes; green densities are high, and the fine particle size promotes sintering.

2. Program Goals

The goals of the program were outlined as:

- a. The development of a fused silica powder suitable for pressing which has fired properties (density, strength, shrinkage, cristobalite content, etc.) similar to slip-cast fused silica.
- b. To develop a fast and efficient method for mixing blends of coarse and fine grain fractions.
- c. To determine whether it is possible to obtain a suitable powder for pressing by spray drying fused silica slip or mixtures

of colloidal silica and fused silica slip mixtures.

- d. To determine what dimensional control can be obtained with isostatic pressing.
- e. To isostatically press a radome shape.
- f. To determine what length forming cycle could be projected for pressing large volumes of fused silica shapes.

## B Experimental Program

### 1. Approach

The program was divided in the phases indicated in Figure 10. Material preparation received primary consideration, starting with the evaluation of grain mixtures and the spray drying of colloidal silica: fused silica slip mixtures. The pressing properties of fused silica powders were evaluated and tooling required to press a radome shape was fabricated.

### 2. Program

#### a. Initial Powder Evaluations

Previous experience at the Engineering Experiment Station with coarse grain fused silica mixtures indicated that a fine (colloidal) particle fraction was needed to provide the sintering necessary to obtain the required densities 16/. To learn what level of additions would be needed with a relatively coarse grain mix, as well as to develop a process for blending the grain and colloidal powders, mixtures of silica grain based on two size fractions (eighty per cent -20 +50 mesh and twenty per cent -325 mesh) were

mixed with Cab-O-Sil<sup>®</sup> M-5 in five ratios of 3, 10, 15, 20, and 30 per cent. These mixtures were placed in one-gallon polyethylene jars and rolled for 48 hours, which significantly reduced the volume of the mix. as the Cab-O-Sil<sup>®</sup> coated the individual fused silica grains. Water additions of 10 w/o (weight per cent) through 16 w/o were made to each powder and the powders again milled for 24 hours.

The powders were precompacted in the molds with a steel plunger, sealed, and isostatically pressed at 5000, 15,000, 25,000, and 30,000 psi in 1/2-inch diameter x 3-1/2-inch long (silastic) rubber molds (Dow Corning RTV<sup>®</sup>) with 1/2-inch thick walls. In each case this produced diametrical laminations causing separation of the pressed bar, with the degree of lamination increasing with higher pressures. The powders were also pressed using 1-inch diameter soft (gooch) rubber tubing. This formed larger cylindrical chips which were still too small for physical measurements.

Experience with these initial trials indicates that in further investigations of Cab-O-Sil<sup>®</sup> water compositions:

- (1) Thin rubber films would be needed for the fabrication of solid cylindrical shapes.
- (2) A pressing pressure of 30,000 psi would be used to obtain maximum green and fired densities.
- (3) Grain compositions containing colloidal silica should be mixed for several days to obtain adequate blending and volume reduction.

#### b. Grain/Cab-O-Sil<sup>®</sup> Mixture Studies

Grain compaction studies showed that a maximum green packing density (1.52 gm/cc) was obtained with a particle size distribution of seventy weight per cent -50 +100 mesh and thirty

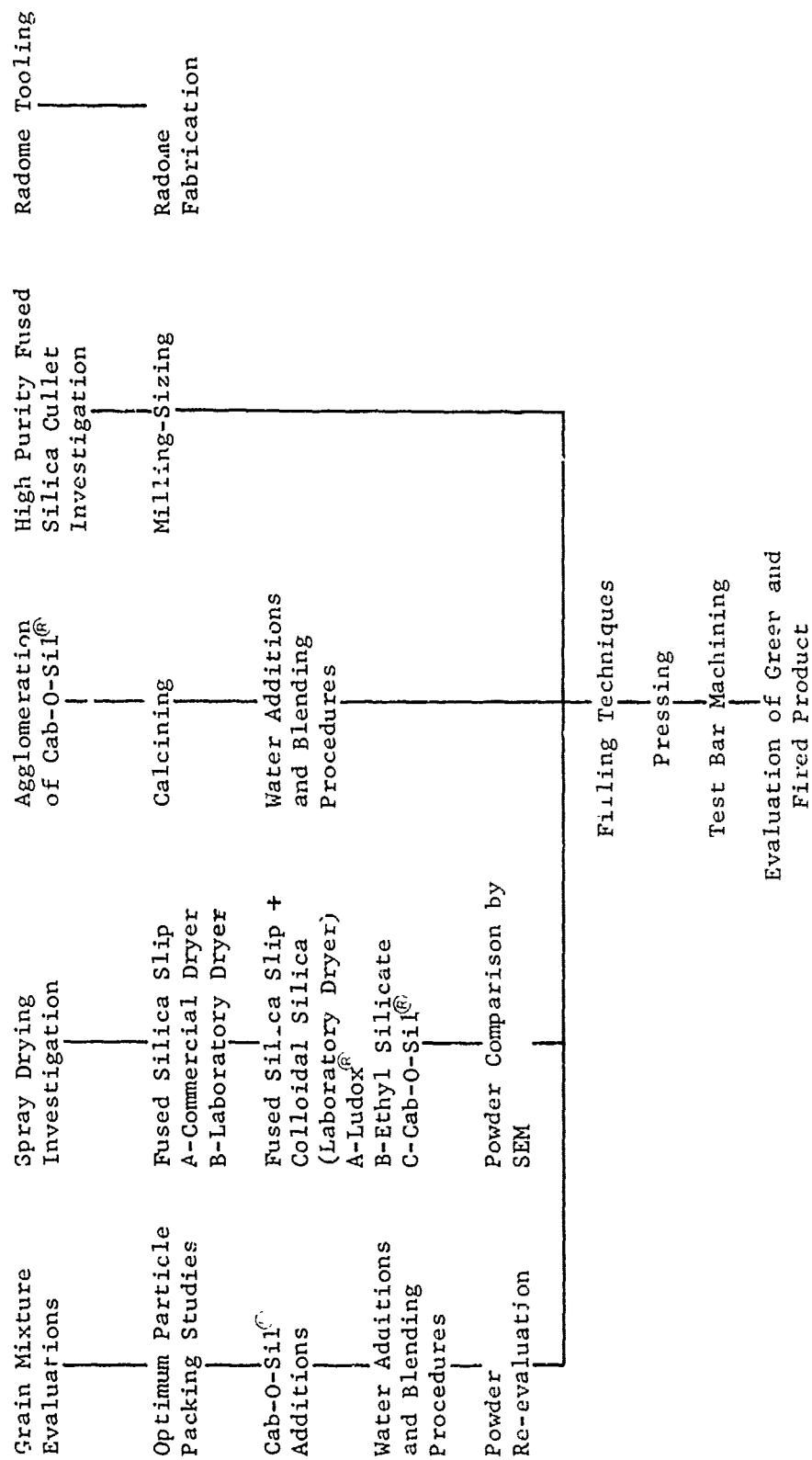


Figure 10. Flow Sheet of Experimental Program for Development of Isostatically Pressed Fused Silica.

weight per cent -325 mesh. Four 1000 gm batches of this mixture were placed in one-gallon polyethylene jars and rolled for 24 hours to assure satisfactory mixing, then Cab-O-Sil<sup>®</sup> L-5 was added in proportions of 20, 25, 30, 35, 40, and 45 per cent.

The Cab-O-Sil<sup>®</sup> L-5 grain mixtures were rolled 72 hours in plastic jars to assure homogeneous mixing, then distilled water additions of 5 to 15 w/o were made to powders containing 20, 25, and 30 w/o Cab-O-Sil<sup>®</sup>. Subsequent pressing trials were unsuccessful because of test bar wafering. The powders receiving 15 w/o water turned into wet pastes, fixing the upper limit for water additions. Grain compositions containing Cab-O-Sil<sup>®</sup> additions of 35, 40, and 45 w/o received water additions of 10 to 13 w/o. Satisfactory solid test bars were pressed from these powders. Bar diameters varied from 1/2-inch to 1-1/4-inch and lengths from 4 to 7-inch, with the damp powder being precompacted in the rubber films before pressing at 30,000 psi. The initial bars were dried at 120° F for 24 hours, then at 350° F for 3 hours before machining; however, subsequent trials were dried by directly placing bars in the higher temperature oven without detrimental effects.

The pressed bars were uneven and required machining to produce an even shape suitable for physical property measurements. Machining was accomplished by mounting the dry bars in a lathe and grinding with a diamond wheel. Attempts to round up the bars using a centerless grinder were unsatisfactory due to grain pull-out.

#### c. Initial Firing and Property Evaluation

Results of physical properties versus firing time and composition are recorded in Table XVI. Symbols identify each composition. For comparison purposes, typical properties of technical grade

TABLE XVI  
 MATERIAL PROPERTIES OF ISOSTATICALLY PRESSED FUSED SILICA TRIAL POWDERS

Firing Time 2300°F (hr)	AB	CD	EF	G	H	I	J	M	N
	Pressed Green Density (30,000 psi)								
	1.36	1.40	1.43	1.35	1.40	1.43	1.34	1.05	~ 1.88
	Fired Density								
	1.75	1.77	1.63	1.40	1.60	---	1.48	1.58	~ 1.90
1.0	Fired Shrinkage (%L)								
	8.6	7.9	7.2	1.2	3.6	---	2.7	14.1	~ 1.0
	E Sonic Modulus (psi x 10 <sup>6</sup> )								
	4.1	3.8	3.77	4.94	4.06	---	5.66	---	~ 3.0
2.25	Fired Density								
	1.93	1.93	1.93	1.45	1.68	1.60	1.48	1.68	~ 1.96
	Fired Shrinkage								
	11.5	9.1	10.1	2.3	6.0	3.6	3.2	15.4	~ 1.5
	E Sonic Modulus (psi x 10 <sup>6</sup> )								
	6.6	4.8	5.7	5.4	---	4.9	---	---	~ 4.0
3.25	Fired Density								
	2.0	1.99	1.97	1.51	1.71	1.61	1.48	1.77	~ 1.97
	Fired Shrinkage								
	12.8	12.7	10.4	3.0	7.9	3.2	3.0	15.7	~ 2.0
	E Sonic Modulus (psi x 10 <sup>6</sup> )								
	6.8	4.9	5.9	1.2	2.8	1.4	---	1.37	~ 4.7
4.25	Fired Density								
	2.04	2.03	1.99	---	1.74	1.62	---	1.80	~ 2.00
	Fired Shrinkage								
	13.2	13.6	11.1	3.4	9.6	3.8	---	16.9	~ 2.0
	E Sonic Modulus (psi x 10 <sup>6</sup> )								
	6.6	---	5.7	---	3.2	3.6	---	2.0	~ 5.0
5.25	Fired Density								
	2.05	2.05	2.02	1.52	1.76	1.62	---	1.84	~ 2.02
	Fired Shrinkage								
	13.6	13.9	11.5	3.8	10.0	3.8	---	17.3	~ 2.0
	E Sonic Modulus (psi x 10 <sup>6</sup> )								
	6.7	---	5.3	1.6	3.6	---	---	---	~ 5.5

Symbol Identification

Base Grain Mixture

70 per cent -50 +100 mesh

30 per cent -325 mesh

A-B 45 per cent Cab-O-Sil<sup>®</sup>

C-D 40 per cent Cab-O-Sil<sup>®</sup>

E-F 35 per cent Cab-O-Sil<sup>®</sup>

G 15 per cent Ethyl Silica, 85 per cent Fused Silica Slip

H 15 per cent Cab-O-Sil<sup>®</sup>, 85 per cent Fused Silica Slip

I 15 per cent Ludox, 85 per cent Fused Silica Slip

J 35 per cent Ludox, 65 per cent Fused Silica Slip

M 100 per cent Cab-O-Sil<sup>®</sup> pelletized and calcined

N Technical grade Slip-Cast Fused Silica (average values).

Spray Dried

Samples pressed with 10-13 per cent water.

slip-cast fused silica are listed in column N. The density versus firing time of these compositions is illustrated graphically in Figures 10 through 14 and fired shrinkage versus firing time is shown in Figures 16 through 19, Appendix II.

Table XVI shows that powder E F has the most desirable combination of properties. Powders A B and C D had higher firing shrinkages because of the higher Cab-O-Sil<sup>®</sup> additions. Powders G through J had low green densities and thus did not reach sufficient fired densities, although firing shrinkage were low. Powder M had excessive firing shrinkage. Powder E F was selected for further investigation, and results shown in Table XVI indicate that fired densities obtained with the pressed powders when fired 4.75 hr @ 2300° F are in the same range as slip-cast material and that the increased shrinkage is related to the lower green densities. The strengths of pressed powders are lower, and may be caused by the larger Griffith cracks associated with the coarser particle size.

However, cristobalite levels are in the range associated with surface cracking due to the volume change from the high to the low form of cristobalite during cooling to room temperature. This could also explain the lower strength. Previous experience with technical grade slip-cast fused silica has indicated that mechanical strength properties were not always predictable with cristobalite levels greater than ten volume per cent.

#### d. Powder Reevaluation

Powders initially investigated (Tables XVI and XVII) showed high (10 per cent) fired shrinkage. To reduce this to the range of slip-cast fused silica (~ 2 per cent), grain size distributions and Cab-O-Sil<sup>®</sup> additives were reevaluated. Table XVII shows the

TABLE XVII

RESULTS OF ISOSTATICALLY PRESSED FUSED SILICA GRAIN  
(POWDER E-F FROM TABLE I)

<u>No. of Samples</u>	<u>Green Density*</u> (gm/cc)	<u>Fired Density</u> (gm/cc)	<u>Fired Shrinkage</u> (%)	<u>MOR</u> (psi)	<u>Cristobalite</u> (%)	<u>Firing</u>	
						<u>Time</u> (hr)	<u>Temp</u> (°F)
5	1.44	1.61	5.41	1372	2.94	4	2210
4	1.48	1.96	7.4	1439	11.7	4.75	2300
Technical Grade Slip- Cast Fused Silica	~ 1.88	~ 2.0	~ 2.0	2000 to 5000	~ 10-15	4.75	2300

\* Pressed @ 30,000 psi.  
 Technical grade grain -  
 70 per cent -50 +100 mesh  
 30 per cent -325 mesh  
 35 per cent Cab-0-Sil<sup>(a)</sup>.

Results are average values of samples tested.

TABLE XVIII  
SUMMARY OF BLENDS 12/

Source	Ref.	Blend	Size 1	Size 2	Size 3	Size 4	Size 5	Type of Particle	Percentage of Theoret. Density Calculated	Density Experimental
Dalla Valle		Tyler Sieve Nos. 74.5	42/48 5.3	100/115 5.3	200/250 1.7	250/270 2.9	270/325 13.6	Uniform spheres*	86.4	
Dayton; Brown		Tyler Sieve Nos. 50 64 65	20/100 9.8 --- ---	100/140 9.8 --- ---	140/200 3.7 9 5	200/235 9 ---	325 22.1 27 30	Fused UO <sub>2</sub> pellets		83.0 86.1 86.6
Webb		Tyler Sieve Nos. 6/20 70 65 65 63	6/20 --- --- --- ---	20/35 --- --- 7.4 ---	-400 30 35 27.6 16.4	---	---	UO <sub>2</sub> pellets		80.8 79.9 82.2 79.3
Hanth		Tyler Sieve Nos. 6/20 67.5 1 1	6/20 12.5 0.023 0.25	35/100 12.5 0.023 0.25	-200 20 0.0005 0.063	---	---	High-density UO <sub>2</sub> Uniform spheres	98.3	92 ---

\*Model systems consisting of spheres of equal density

Table XVI shows the results of powder compaction densities obtained by several workers

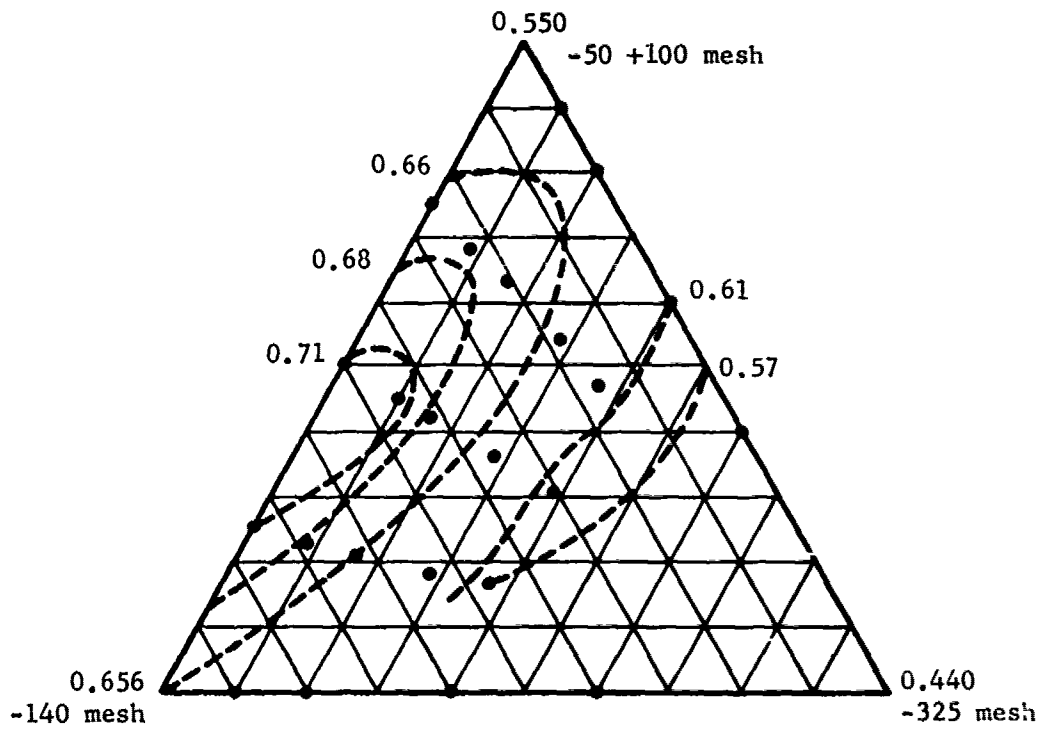
results of powder compaction densities obtained by several workers, and Table XVIII gives results of compaction studies with fused silica grain of varying particle size distributions. Trial A-1 shows the packing density obtained with a theoretically optimum size distribution for spherical shot as reported by McGearry 12. Additions of finer size fractions in subsequent trials produced increasingly higher densities, which reached a maximum of 1.59 gm/cc. Trial B of Table XIX shows that a significantly lower density (1.28 gm/cc maximum) is obtained if the -140 mesh addition is eliminated from the three mesh sizes used in Trial A. Work with the -20 +50 mesh size was not carried further because the coarse grain produced an unacceptably rough pressed surface. Trial C, using a -50 +100 mesh size as the coarse fraction, produced a maximum density (1.51 gm/cc) with 30 per cent -325 mesh grain, and the addition of -140 mesh grain (Trial D) gave a slightly higher value (1.54 gm/cc). Trial E indicated lower density (1.37 gm/cc) resulted when -50 +200 mesh was substituted for the -50 +100 coarse fraction.

The above compaction determinations were made by filling a 100 ml volumetric cylinder with the powder mix, tapping the cylinder on the table top until settling stopped, then refilling and again tapping. It was found that tapping produced denser packing than vibrating at the frequency of the available laboratory vibratory table, and was considered satisfactory for comparative purposes. The weight of the filled cylinder minus the tare was considered to be the maximum density of the grain mix.

Figure 11 shows results of a particle packing study designed better to define optimum volumes for available grain sizes which give acceptable surface finish.

TABLE XIX  
 PACKING DENSITY OF VARIOUS GRAIN SIZE DISTRIBUTIONS  
 (100 ML GRADUATED CYLINDER TAPPED ON TABLE UNTIL SETTLING STOPPED AND CYLINDER FULL)

Mesh Size	-20 +50 (%)	-50 +100 (%)	-100 +200 (%)	-140 (%)	-325 (%)	Density (gm/cc)	Per Cent of		Comment
							Theoretical		
Trial A	1 66	26 9	31 11	35 14	38 16	1.49	0.68	Distinct segregation of fines and coarse fraction	
	2 58					1.53	0.70	Distinct segregation	
	3 51					1.55	0.71	Less distinct segregation	
	4 46					1.59	0.72	Segregation slight - entrapped air causes mix to bounce when initially tapped. Coarse grain produced rough surface on pressed bars.	
Trial B	1 100					1.16	0.53		
	2 95				5	1.21	0.55		
	3 90				10	1.25	0.57		
	4 85				15	1.26	0.57		
	5 80				20	1.28	0.58		
	6 75				25	1.26	0.57		
Trial C	1 80				20	1.46	0.66		
	2 70				30	1.51	0.69		
	3 60				40	1.43	0.65		
	4 50				50	1.29	0.59		
Trial D	1 100					1.19	0.54		
	2 67		25		8	1.42	0.65		
	3 58		31		11	1.51	0.69		
	4 51		35		14	1.54	0.70		
Trial E	1 100					1.10	0.50		
	2 66		25		8	1.30	0.59		
	3 59		30		11	1.37	0.62	Discontinued because density low.	



\*/ Isodensity Mixtures Shown by Dashed Lines Indicate Per Cent Theoretical Density ( $2.20 \text{ gm/cm}^3$ ).

Figure 11. Ternary Packing Equilibrium Diagram for Fused Silica Grains.

Each point is an average of five values, obtained by filling five 100 ml volumetric cylinders with 70 grams of grain each, then vibrating for five minutes. The standard deviation of sample densities was less than 5 per cent. The grain was pre-blended prior to vibrating by rolling in a plastic jar. To promote sintering, a grain mixture containing the maximum volume of -325 mesh consistent with good packing densities (Trial D-3, Table XIX) was selected for pressing.

Cab-O-Sil<sup>®</sup> was added to the above grain mixtures by tumbling in a rotating drum of V-type laboratory blender.

#### e. Binder Evaluation

Powders of the compositions shown in Table XVIII resembled dry beach sand and would not form a cohesive pressed shape before water and/or a binder was added. After comparing several commercial binders (PVA<sup>®</sup>, Carbowax<sup>®</sup>, starch), a 1.0 per cent Methocel<sup>®</sup>-water solution was found to give sufficient green strength after pressing to permit dry machining of test bars.

The binder solution was most satisfactorily added in a laboratory V-type blender equipped with a liquid dispersing bar. This produced a fairly uniformly pelletized product which would flow into a mold. Moisture levels of 6 per cent gave adequate green strengths, and test bars (1.0 inch in diameter) could be dried quickly (~2 hours) by placing them directly into a 300° F oven.

#### f. Pressing Procedures

All powders were contained in a sealed flexible (rubber) mold, pre-compacted by tapping and in some cases evacuated, then isostatically pressed at 30,000 psi. It was not possible to

distinguish between pressed bars which were or were not evacuated prior to pressing. Test bars ~ 1.0-inch diameter x 6.0 inches long were the principal shape pressed because bars were needed for mechanical evaluation. It was learned that a stiff-walled rubber tube (1/16-inch thick rubber resembling the stiffness of rubber bands) tended to diametrically fracture the pressed bars in wafer-like pellets. Bars did not wafer if a thin-walled pliable rubber was used or if the pressed strength was sufficiently high.

A more promising procedure for forming test bar shapes is to position a metal mandrel in a thicker-walled rubber tube. This eliminates the wafering and also produces a bar of more uniform outside dimension. The mandrel can be easily removed from the pressed shape, and strength and shrinkage calculations altered to allow for the hollow test bar. Some problem occurred due to bending of the mandrel during pressing. This prevented removal of the mandrel without breaking the pressed sample.

#### g. Pressed Powder Evaluations

Table XX shows green density and fired properties of fused silica powders based on a mix of 51 per cent -50 +100 mesh, 35 per cent -140 mesh, and 14 per cent -325 mesh grain. Initial tests without Cab-O-Sil<sup>®</sup> gave low fired densities, so increasing amounts of Cab-O-Sil<sup>®</sup> were added to increase sintering activity and density, and yet maintain lower shrinkage than previous powders.

Trends shown by Table XX are:

- (a) Green density decreased with increasing Cab-O-Sil<sup>®</sup> content.
- (b) Fired densities, shrinkage, and strength increase with higher Cab-O-Sil<sup>®</sup> content when fired for 4.5 hours at 2300° F.

TABLE XX  
 MATERIAL PROPERTIES OF ISOSTATICALLY PRESSED FUSED SILICA PADDERS  
 WITH INCREASING CAB-O-SIL CONTENT

	Per Cent Cab-0-Sil <sup>a</sup>					Slip-Cast Fused Silica (Technical Grade) <sup>b</sup>
	0	5	10	20	30	40
Green Density (pressed at 30,000 psi)	1.60	1.61	1.61	1.56	1.37	1.37
Fired Density (2300° F)	4.5 hr	1.74	1.78	1.84	1.85	~ 1.88
	6.7 hr	1.78	1.84	1.89	1.84	~ 2.0
Fired Shrinkage (%)	4.5 hr	1.47	3.4	5.3	9.4	~ 2.0
	6.7 hr	2.32	2.7	2.9	4.42	---
E Modulus of Elasticity (psi x 10 <sup>6</sup> )	4.5 hr	---	1.35	1.95	2.29	~ 5.0
	6.7 hr	1.04	1.09	0.94	1.3	---
Modulus of Rupture (psi)	4.5 hr	323	670	1281	1261	~ 4500
	6.7 hr	---	---	---	---	---
Cristobalite (%)	4.5 hr	---	15.4	13.1	9.5	10-15
	6.7 hr	22.1	26.1	24.2	20.8	---

<sup>a</sup> Average values.

Above values based on 1 to 4 samples.

Above bars pressed with ~ 5 per cent moisture - added as 1 per cent methocel solution to grain mixtures.

Symbol identification

Base grain mixture

mesh	per cent
-50 +100	51
-140	35
-125	14

0	5	10	20	30	40
Per Cent Cab-0-Sil <sup>b</sup> added to above grain.					

- (c) Cristobalite content decreases with increasing Cab-O-Sil<sup>®</sup>.

h. Cab-O-Sil<sup>®</sup> Agglomeration

The relatively coarse, angular particles characteristic of fused silica grain are not the optimum shape to obtain dense pressed shapes. Silica is also commercially available in the form of colloidal powders (Cab-O-Sil<sup>®</sup>), and trials were conducted to determine if granular powders more suitable for pressing than fused silica grain could be made from this material.

Initially, a 17 w/o Cab-O-Sil<sup>®</sup>-water mixture was prepared and rolled in a plastic jar. Cab-O-Sil<sup>®</sup> additions were made at two-hour intervals until pellets of 1/2- to 3/4-inch diameter were formed. These were broken up and rolling continued for 48 hours, resulting in small spheres.

To reduce the fired shrinkage of the colloidal powder the following processing procedure was followed:

- (a) Sintering of small spherical powders at 1800, 1900, and 2000° F.
- (b) Ball milling (15 minutes maximum).
- (c) Distilled water additions (10 per cent).
- (d) Blending (Rolling in plastic cylinder 24 hr.).
- (e) Pressing in soft rubber (gooch) tubing at 30,000 psi.
- (f) Firing (4 hours at 2200° F).

The resulting low densities (1.3 gm/cc) and high fired shrinkages (30-35 per cent) indicate it would be difficult to equal the green densities or fired shrinkages of slip-cast fused silica using a pressed grain made as outlined above.

### i. Spray Drying

The physical properties (bulk density, particle distribution, flowability, etc.) of spray-dried powders are subject to considerable variation and are dependent on the properties of the feed material (solids content, viscosity, solid characteristics, etc.) as well as the design (type of atomization, dryer size, direction of air flow, etc.) and operation (temperatures, feed rates, volume of air flow, etc.) of the dryer. Reviews of spray dryer design and operation are given by Perry 14/ and Marshall 15/.

The principal advantages of spray dried ceramic powders for isostatic pressing are that powder packing density can be improved if dense spherical particles of optimum particle size distribution can be formed, powder flowability is good, pressing moisture levels can be low, and binders for improving green strength can be added prior to spray drying.

Recovery rates with the fused silica slips were approximately 85 per cent, while trials with the high colloidal particle content (Trials 6 and 7, Table XXI gave low (15 per cent) recovery ratio with a high stack loss.

The powders obtained from laboratory dryer trials were typically fine and fluffy, flowed poorly, and pressed to low green densities, thus resulting in low fired densities. Green and pressed results with these powders are shown in Table XVI. Water additions (10 per cent) were made to the powders to improve pressed green strength; however, the unfired bars were fragile and difficult to machine.

Several gallons of slip were sent to Bowen Engineering to determine if an improved powder granulation and thus packing densities could be obtained with a larger spray dryer. Results of these trials show that a larger commercial dryer will produce

TABLE XXI  
 TRIALS MADE WITH THE EES LABORATORY  
 SPRAY DRYER

	(Weight Per Cent of Total Silica)						
	<u>1</u>	<u>2</u>	<u>3</u>	<u>4</u>	<u>5</u>	<u>6</u>	<u>7</u>
Fused Silica Slip	100*	85	85	85	35		
Ethyl Silicate		15					
Cab-O-Sil <sup>(R)</sup> L-5			15			80	10
Ludox <sup>(R)</sup> Ammonia Stabilized				15	65	20	90

All solutions diluted 100 per cent by volume with distilled water to lower viscosity.

\* Tested both diluted and undiluted.

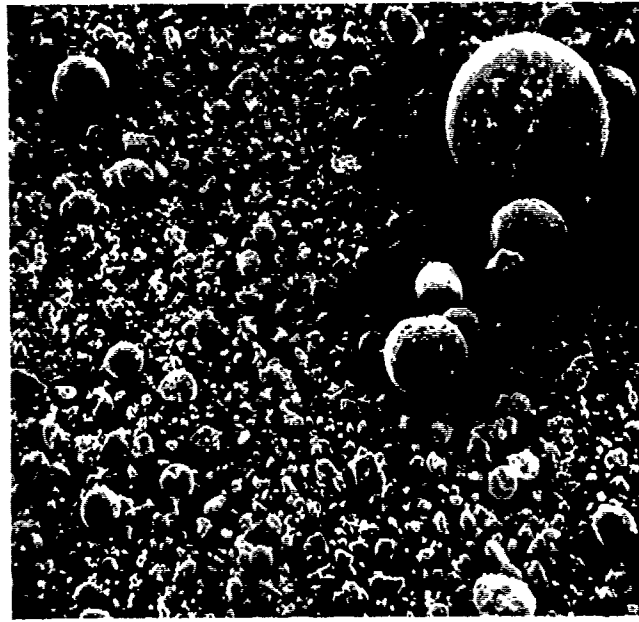
Typical dryer control settings were:

Inlet temperature	550° F
Outlet temperature	290° F
Air pressure	100 psi
Feed rate	2 gal/hr

spherical particles from fused silica slip. Bowen engineers report that such granulation is often difficult to obtain with a laboratory size spray dryer. Some fines were collected in the cyclone of the commercial dryer, and it is unknown to what degree the particle size distribution of the granular product collected in the dryer chamber was changed from that of the original slip. One trial was also made with slip to which 2 per cent Carbowax<sup>®</sup> had been added.

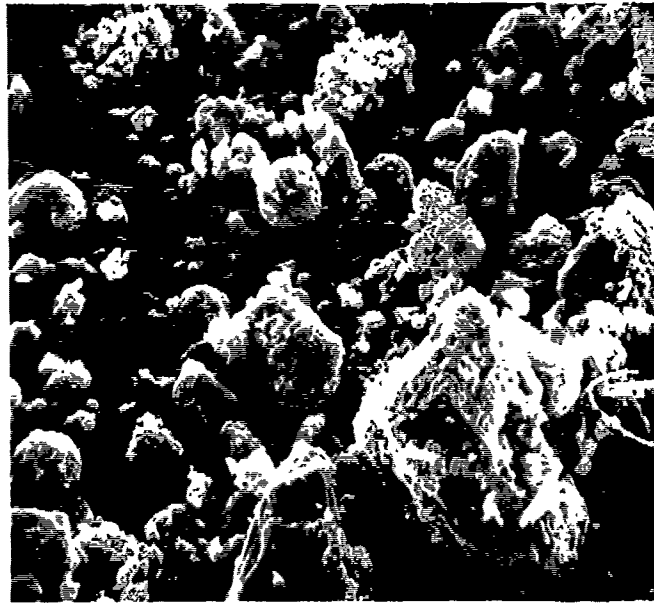
Scanning electron micrographs were taken of the powders produced by Bowen as well as those made at Georgia Tech. Figure 12 shows the difference in granulation of the Bowen powders collected in the cyclone and in the chamber, using a slip containing 2 w/o Carbowax<sup>®</sup>. The large spheres shown in the top micrograph range from 25 to 150 micrometers. However, an undesirably high fine content is also observed. The largest particle collected in the cyclone, shown in the bottom micrograph, is approximately 30 micrometers. Figure 13 shows that spray dried fused silica powder produced at Georgia Tech has a particle size range of approximately 1 to 10 micrometers and poor agglomeration. Figure 14 shows fine spherical particles obtained with the Georgia Tech laboratory dryer with a solution of 90 per cent Ludox<sup>®</sup> and 10 per cent Cab-O-Sil<sup>®</sup>. This mixture flowed more evenly than fused silica slip and the spray dried results indicate better atomization was obtained.

Results with the spray dried powders received from Bowen Engineering were inconclusive. Several dryer adjustments produced small samples of 3 powders, which limited the number of bars which could be pressed, and the bars which were pressed had low green strength. This problem should be solvable by addition of a suitable binder in the slip and/or by optimizing the spray drying process.



100  $\mu$ M

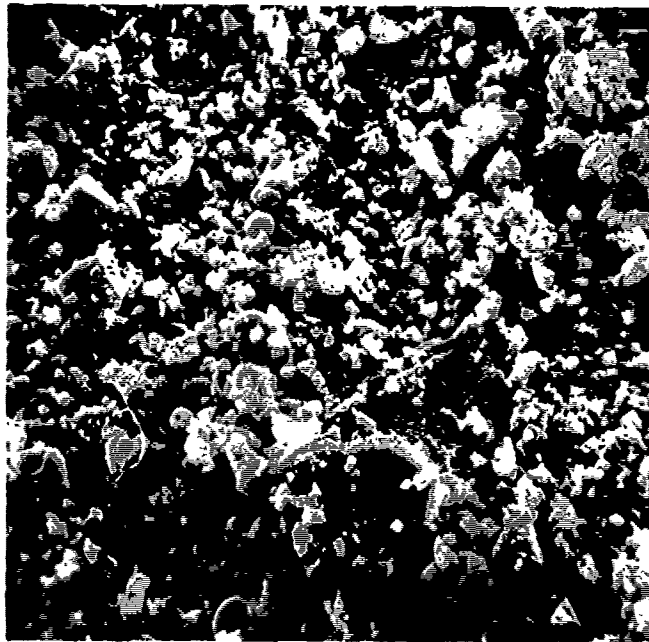
a. Chamber Collected



100  $\mu$ M

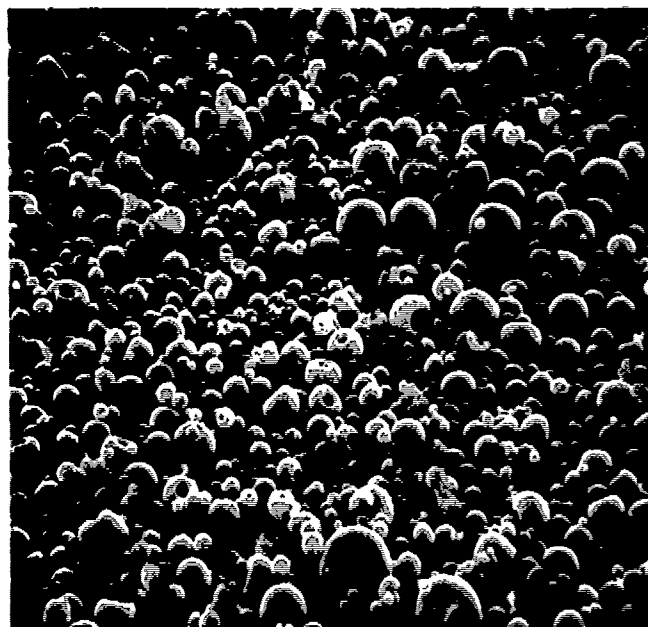
b. Cyclone Collected

Figure 12. Scanning Electron Micrograph of Bowen Powders Containing 2 weight per cent Carbowax



100  $\mu\text{M}$

Figure 13. Scanning Electron Micrograph of Spray Dried Fused Silica Slip Collected at Georgia Tech



100  $\mu\text{M}$



10  $\mu\text{M}$

Figure 14. Scanning Electron Micrograph of 90 weight per cent Silica from Ludox - 10 per cent Cab-O-Sil L-5

Because of the low green strength, dry machining was difficult, and fired results were obtained on only two small bars. These results were contradictory and indicated more work is needed to adequately evaluate powders prepared by spray drying fused silica slips.

j. High Purity Fused Silica Grain Mixtures

Experience with slips made from high purity fused silica cullet at Georgia Tech shows that this material sinters more easily, with lower cristobalite content, than slips made from technical grade fused silica 13/. Because of these advantages, high purity glass cullet was ground (See Appendix III for procedures followed) and grain mixtures made similar to those previously evaluated.

A comparison of initial results is given in Table XXII. The high purity material shows an anomalously high cristobalite content.

Comparative chemical analysis of the fired bars made from high purity grain and high purity slip-cast fused silica is shown in Table XXIII.

The higher Na, K, MgO, and CaO values obtained with the high purity grain account for the high cristobalite content. The higher  $Al_2O_3$  content of the slip is picked up by the long (several hours) grinding in alumina ball mills and is not detrimental. The increased contamination undoubtedly came from the glass cullet grinding operation, and this trial should be repeated under improved experimental conditions.

Also, further trials are needed to evaluate the high purity grain at shorter firing times.

---

\* High purity fused silica refers to slips or grain made from high purity fused silica glass cullet rather than technical grade fused silica obtained from the crude arc fusion of silica sand.

TABLE XXII  
ISOSTATICALLY PRESSED HIGH PURITY FUSED  
SILICA GRAIN MIXTURES

	Firing Time (2300° F)	
	<u>High Purity Grain</u>	<u>Technical Grain</u>
	4.75 hr	4.75 hr <sup>(d)</sup>
Green Density (gm/cc)	1.41 <sup>(b)</sup>	1.48
Fired Density (gm/cc)	1.95 <sup>(b)</sup>	1.96
Fired Shrinkage %ΔL	10.1 <sup>(b)</sup>	10.5
MOR (psi)	800 <sup>(c)</sup>	1440
Cristobalite (%)	~ 70 <sup>(c)</sup>	11.7

(a) powder based on 70 per cent -50 +100 mesh; 30 per cent -325 +35 per cent Cab-O-Sil<sup>®</sup> addition: bars pressed @ 30,000 psi.

(b) Based on average of 5 solid bars.

(c) Based on average of 2 solid bars.

(d) Based on average of 4 solid bars.

TABLE XXIII

COMPARATIVE SPECTROGRAPHIC ANALYSES OF PRESSED HIGH  
PURITY GRAIN AND SLIP-CAST FUSED SILICA

---

	<u>High Purity Grain (Weight %)</u>	<u>High Purity SCFS (Average Weight %)</u>
Na	.02	.004
K	.02	.001
Li	.002	.001
Al <sub>2</sub> O <sub>3</sub>	.18	.323
TiO <sub>2</sub>	.004	.004
Fe <sub>2</sub> O <sub>3</sub>	.008	.013
MgO	.019	.010
CaO	.019	.011
*SiO <sub>2</sub>	99.73	99.64

---

\* By difference

---

#### k. Radome Tooling and Pressing

Tooling designed to press a cone approximately 6 inches high by 5 inches in diameter is shown in Figure 15. This permitted the interior conical mandrel to be positioned while powder was being poured into the space between the outer bag and the mandrel, provided support and a seal for the filled bag, and permitted evacuation before pressing. The filled bag remained in the perforated outer support during pressing. Initial results with radome shapes pressed with the tooling shown in Figure 15 were encouraging. For pressing procedures used see Appendix IV.

The wall thickness of these shapes was relatively uniform, and interior dimensions of the green part can be held to close tolerances because pressing is done against a mandrel. Outside tolerances are controlled by powder packing densities prior to pressing and pressing pressure, parameters which should become uniform after powder preparation, filling procedures, and pressing pressures have been standardized.

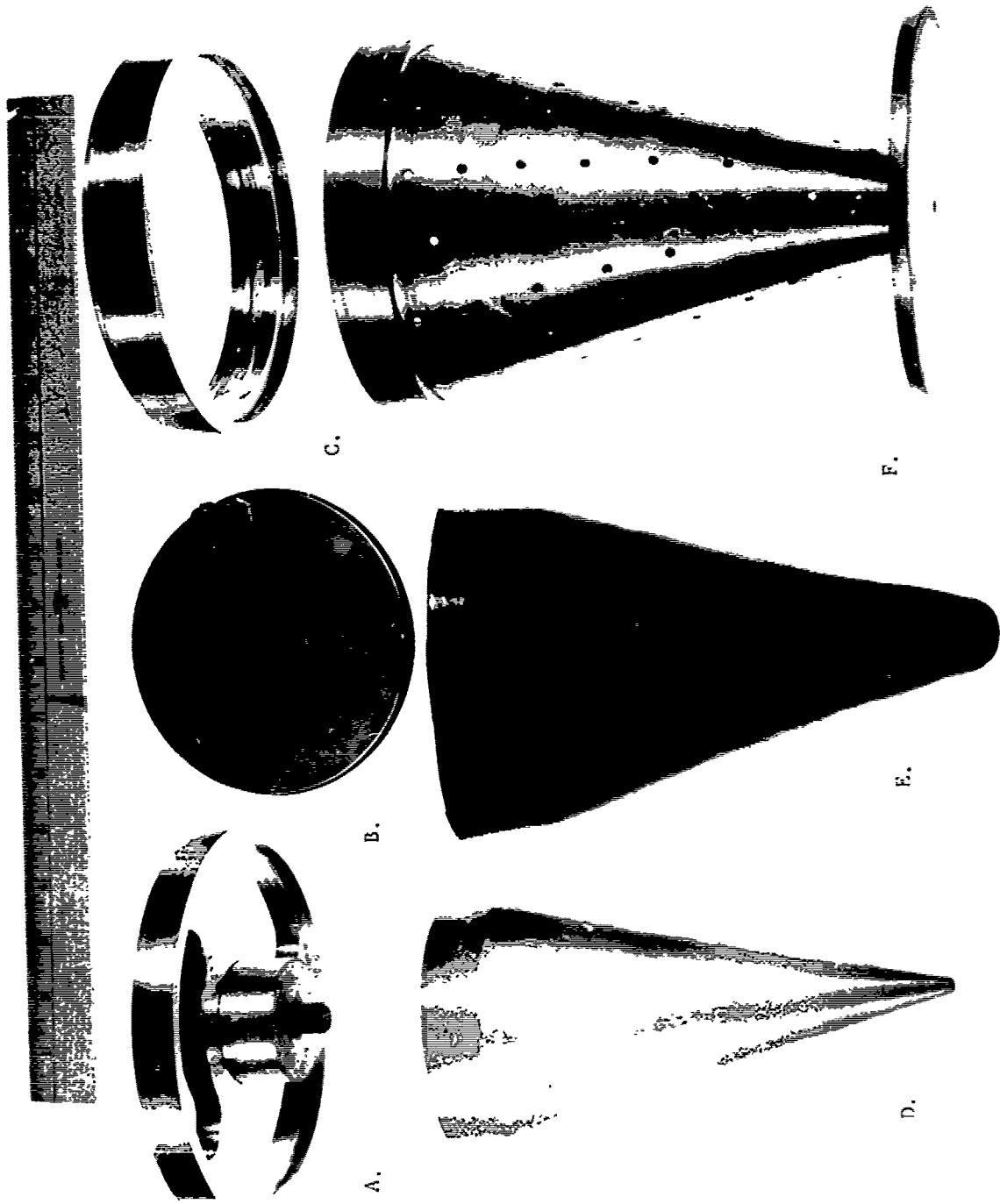


Figure 15. Tooling Used to Isostatically Press Radome

## C. Discussion

### 1. Powder Preparation

Green packing densities of slip-cast fused silica and the best fused silica grain mixtures show values of approximately 85 and 70 per cent theoretical density, respectively. This indicates that to improve fired density, shrinkage, and strength of pressed powders we must first obtain better green densities with fused silica grain mixtures. The best pressed densities show values of about 73 per cent theoretical, indicating that pressed density is principally controlled by the packing characteristics of the grain mixture. Fired properties of the pressed powders show that Cab-O-Sil<sup>®</sup> additions are needed to promote sintering required to obtain reasonable fired densities, even though these additions lower green pressed densities and increase shrinkages. Cab-O-Sil<sup>®</sup> also performed as a green binder. Improved green packing densities would improve sintering properties, and thus reduce the necessary Cab-O-Sil<sup>®</sup> additions. Blending Cab-O-Sil<sup>®</sup> and grain mixtures is somewhat difficult, and thorough mixing was found to be necessary.

The characteristics of agglomerated colloidal silica (Cab-O-Sil<sup>®</sup>) powder show that considerably more pre-sintering is needed to reduce the fired shrinkage to reasonable levels. It is known from previous work at Georgia Tech 16/ that high grade fused silica can be produced from such powders. Therefore, it may be possible to produce fused silica spheres with this technique which would have better packing characteristics than the angular particles obtained by grinding fused silica.

## 2. Spray Drying

Fused silica slip shows non-Newtonian (dilatant) flow characteristics which would impair flowability through a spray dryer atomizer. However, the slip mixtures made from colloidal silica (Cab-O-Sil<sup>®</sup> and Ludox<sup>®</sup>) were Newtonian, and fine spherical powders were produced. This indicates that it may be desirable to evaluate slip additives which would improve flow characteristics, then dry these slips in a larger dryer such as the one used by Bowen Engineering to obtain a spherodized product.

## 3. High Purity Fused Silica Grain

The high cristobalite levels shown with the high purity grain mixtures are probably caused by contaminants introduced in the grinding operation. It would seem reasonable to repeat this test with cullet ground in high alumina ball mills, or in some other way thoroughly clean the cullet prior to firing.

## 4. Pressing of Radome Shapes

The tooling initially designed to press a radome shape should be modified to improve the seal between the cap and rubber bag because leaking in this area was a problem. The present tooling is suitable for forming numerous test shapes which could be used to establish approximate forming times, green trimming procedures, and firing tolerances.

## D. Conclusions

1. The work to date indicates a radome shape can be formed by isostatic pressing.
2. The fired properties of pressed fused silica are closely related to the packing and sintering characteristics of the powder

compositions. The properties of pressed fused silica tested so far do not equal those of slip-cast fused silica. More work is needed to develop a powder with a satisfactory particle size distribution which will press to the required densities. Initial tests indicate that spray drying of fused silica slip in a large spray dryer may be a feasible way to prepare such a powder.

E. Author's Opinion of the Isostatic Process as an Alternative Forming Process for Fused Silica Radome Shapes:

Isostatic pressing would offer the most potential in the situation that required rapid fabrication of relatively large numbers (several hundreds) of a particular radome. The initial costs of tooling and pressure vessels must be balanced by the time saving projected, however, the technology and equipment are available.

Cycles of 30 minutes per radome should be possible with relatively simple tooling and commercially available pressure vessels. Assuming a suitable powder is available and that tooling design has been worked out, a rejection rate of 10 to 20 per cent would be estimated as reasonable. This estimate is based on experience with the isostatic forming of toilet tanks and electrical porcelain blanks.

Spray drying of fused silica slip in a large dryer, based on initial tests, appears to offer good potential for powder preparation. Two questions need to be answered; (A) can the particle size distribution of the slips be retained; (B) can the granular powder be pressed to sufficiently high density to give sintered properties similar to slip cast fused silica?

Spray drying is a well developed process, so it seems reasonable to expect that stack losses in a large, properly adjusted dryer would not be severe. It is reportedly possible to spray dry solid granules (the granules obtained on initial trials were hollow), which would

increase powder density and thus reduce the compaction required during pressing. Binder additions can be made to improve green strength, and might also provide lubrication during pressing.

If drying conditions can be found which produce a satisfactory powder, then it should be possible to supply a consistent powder in production quantities at relatively low costs.

Based on experience with the successful spray drying of porcelain slips, and the favorable appearance of the granular powders obtained during initial trials with fused silica slip spray dried in a large dryer, the process appears feasible.

The above is the basis of our statement in the abstract, "the isostatic pressing process has potential but further development is still needed."

#### F. Recommendations for Future Work

1. Packing studies with fused silica grain indicate that it is difficult to obtain packing densities higher than  $\sim 0.72$  theoretical, while slip-cast fused silica has densities of  $\sim 0.85$  theoretical. It would be desirable to combine the packing densities of slip with the rapid forming possible with isostatic pressing. This could possibly be done by:

- a. Substituting the solid mandrel shown in Figure 14 with a strong but porous material, i.e., porous metal;
- b. Covering the porous mandrel with filter paper or other suitable material;
- c. Filling the cavity with slip rather than powder, then sealing;
- d. Pressing (30,000 psi).

This should result in a green casting with:

- (1) Lower moisture than plaster castings;
- (2) Rapid forming.

2. High purity fused silica spheres made from colloidal powders may permit a final product with unique purity and green packing densities of  $\sim 0.85$  theoretical. The technology is available for making these pellets, and experience shows 16/ that raw material purity is influential in controlling the sintering and final physical properties of rebonded fused silica.

3. Green fused silica parts could be processed more easily if their strength was higher and if sufficiently strong, could be machined prior to firing. Therefore, a thorough evaluation of commercial binders may be rewarding.

4. Spray drying appears to offer good potential for powder preparation. This process should be evaluated to determine:

- a. Optimum particle size distribution of dried spheres;
- b. Optimum particle density;
- c. Minimum loss of fine fraction.

Spray dried powders may offer the filling, pressing, and sintering properties needed for isostatic forming. However, a suitable green binder would be required to increase green strengths.

APPENDIX I  
SINTERING DATA FOR SILICON CARBIDE/SILICA COMPOSITES



TABLE XXIV (Continued)  
SINTERING DATA FOR SILICON CARBIDE/SILICA COMPOSITES

Additive Composition	Volume Per Cent Additive	Sintering Time (hr)	Bulk Density (gm/cc)	Packing Efficiency (%)	Per Cent Change in Bulk Density	Per Cent Change in Weight	Per Cent Linear Shrinkage	Tensile Strength (psi)
All A	10	Dry	1.928	82.94	---	---	---	---
		2.33	1.986	85.44	2.98	0.002	0.785	3240
		4	1.984	85.37	3.14	0.068	0.864	3010
		6	1.994	85.79	3.26	0.136	0.753	2830
All E	10	8	1.983	85.34	2.87	0.151	0.800	---
		Dry	1.834	78.93	---	---	---	---
		2.33	1.936	83.29	5.45	0.600	1.373	4650
		4	1.949	83.86	6.57	0.930	1.284	4790
1/3 2/3	10	6	1.984	85.40	8.46	1.285	1.995	4450
		8	1.986	85.45	8.26	1.309	1.684	4330
		Dry	1.904	81.92	---	---	---	---
		4	1.960	84.33	2.82	0.196	0.788	---
2/3 1/3	10	7	1.959	84.28	3.05	0.412	0.712	---
		8	1.960	84.60	3.38	0.448	0.810	---
		Dry	1.918	82.52	---	---	---	---
		4	1.971	84.79	2.96	0.099	0.845	---
1/3 2/3	10	7	1.972	84.87	2.61	0.224	0.751	---
		8	1.974	84.96	2.88	0.309	0.755	---
		Dry	1.884	81.07	---	---	---	---
		4	1.974	84.94	5.05	0.531	1.375	3670
1/3 2/3	10	7	1.993	85.75	5.96	0.838	1.347	4040
		8	1.993	85.74	5.84	1.035	1.304	3870

(Continued)

TABLE XXIV (Continued)  
SINTERING DATA FOR SILICON CARBIDE/SILICA COMPOSITES

Additive Composition	Volume Per Cent Additive	Sintering Time (hr.)	Bulk Density (gm/cc)	Packing Efficiency (%)	Per Cent Change in Bulk Density	Per Cent Change in Weight	Per Cent Linear Shrinkage	Tensile Strength (psi)
2/3 1/3	10	Dry	1.909	82.15	---	---	---	---
		4	1.989	85.58	4.17	0.304	1.090	---
		7	1.992	85.70	4.34	0.559	1.027	---
		8	1.991	85.67	4.28	0.655	1.043	---
1/3 2/3	10	Dry	1.868	80.37	---	---	---	---
		4	1.980	85.18	5.91	0.639	1.491	4420
		7	1.987	85.48	6.46	1.090	1.482	3770
		8	1.987	85.50	6.37	1.267	1.435	3690
2/3 1/3	10	Dry	1.883	81.03	---	---	---	---
		4	1.964	84.50	4.36	0.542	1.127	---
		7	1.967	84.64	4.32	0.835	0.986	---
		8	1.964	84.50	4.37	0.953	0.989	---

APPENDIX II

GRAPHICAL REPRESENTATION OF DENSITY AND SHRINKAGE  
VERSUS FIRING TIME (2300° F) FOR ISOSTATICALLY PRESSED POWDERS

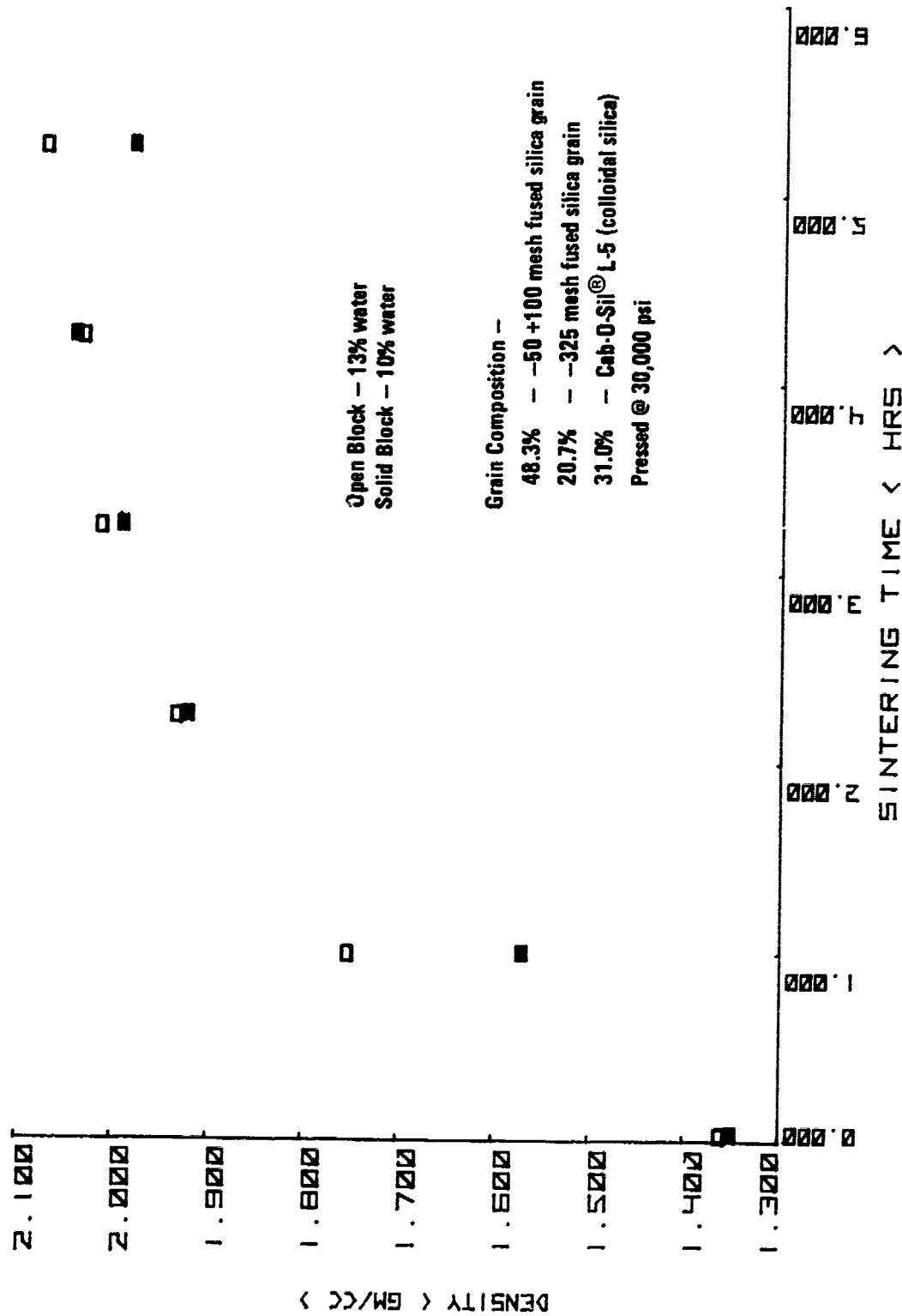


Figure 16a. Density Versus Sintering Time @ 2300°F

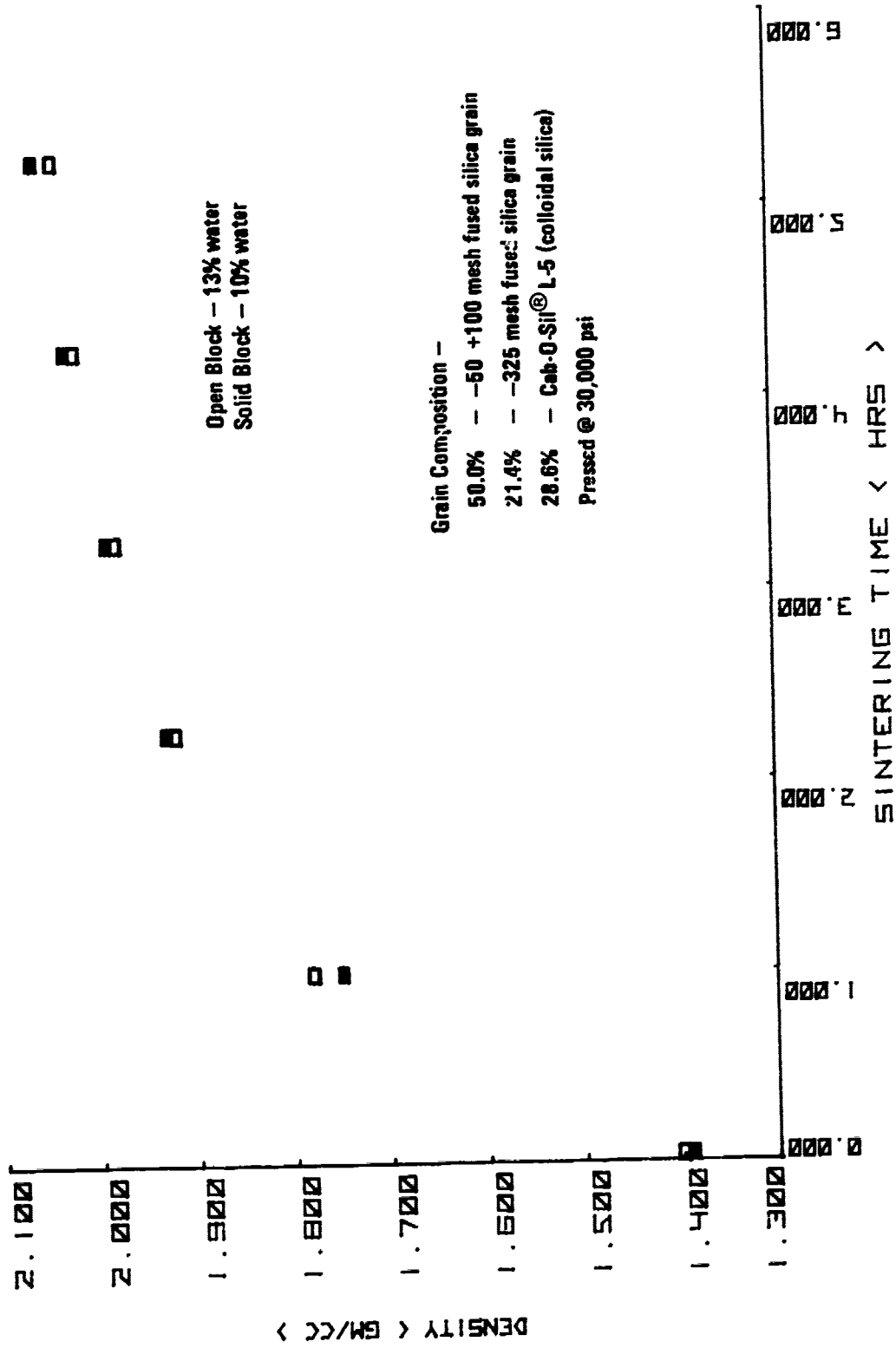


Figure 16b. Density Versus Sintering Time @ 2300°F

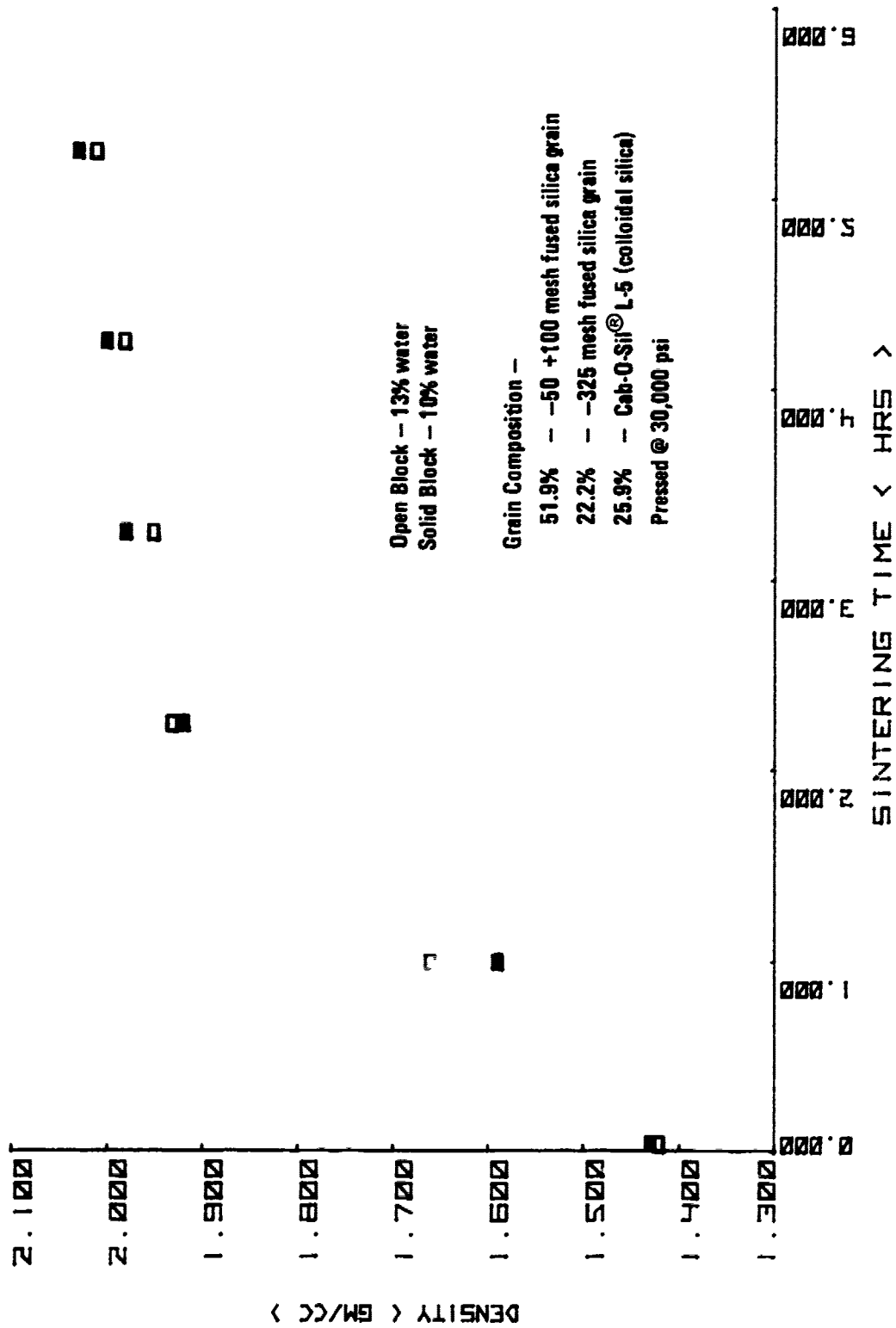


Figure 16c. Density Versus Sintering Time @ 2300°F

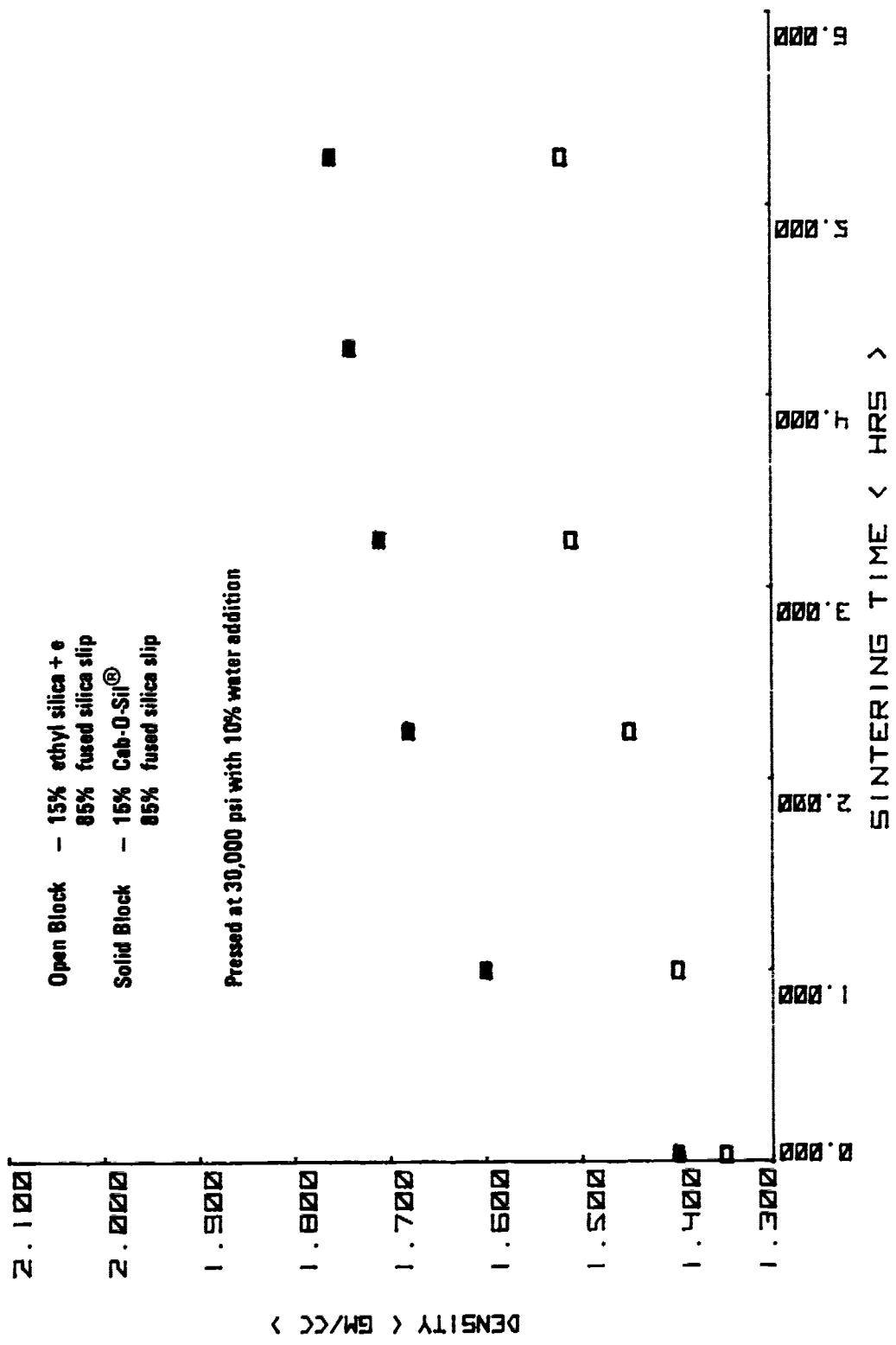


Figure 16d. Density Versus Sintering Time @ 2300°F

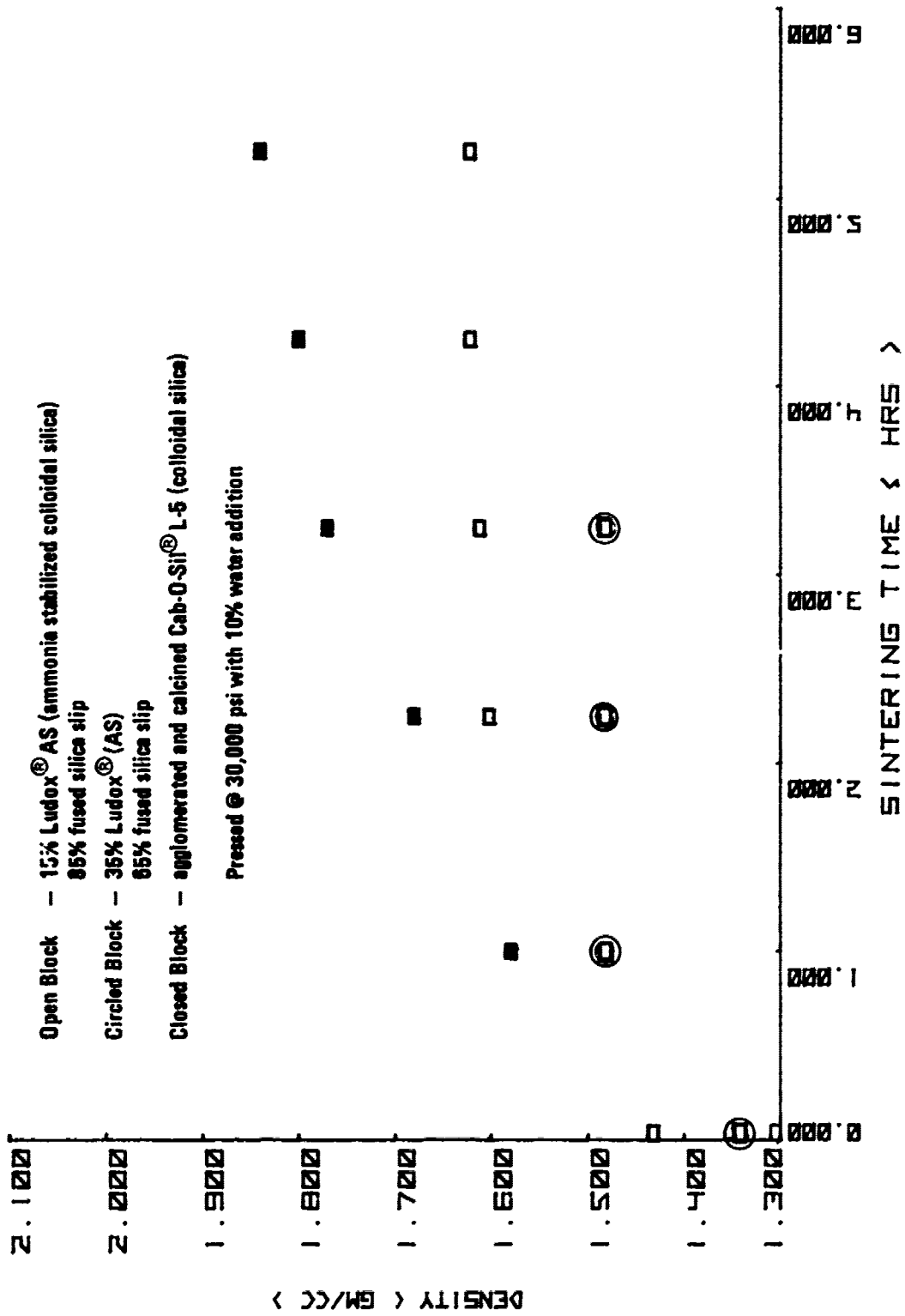


Figure 16e. Density Versus Sintering Time @ 2300°F

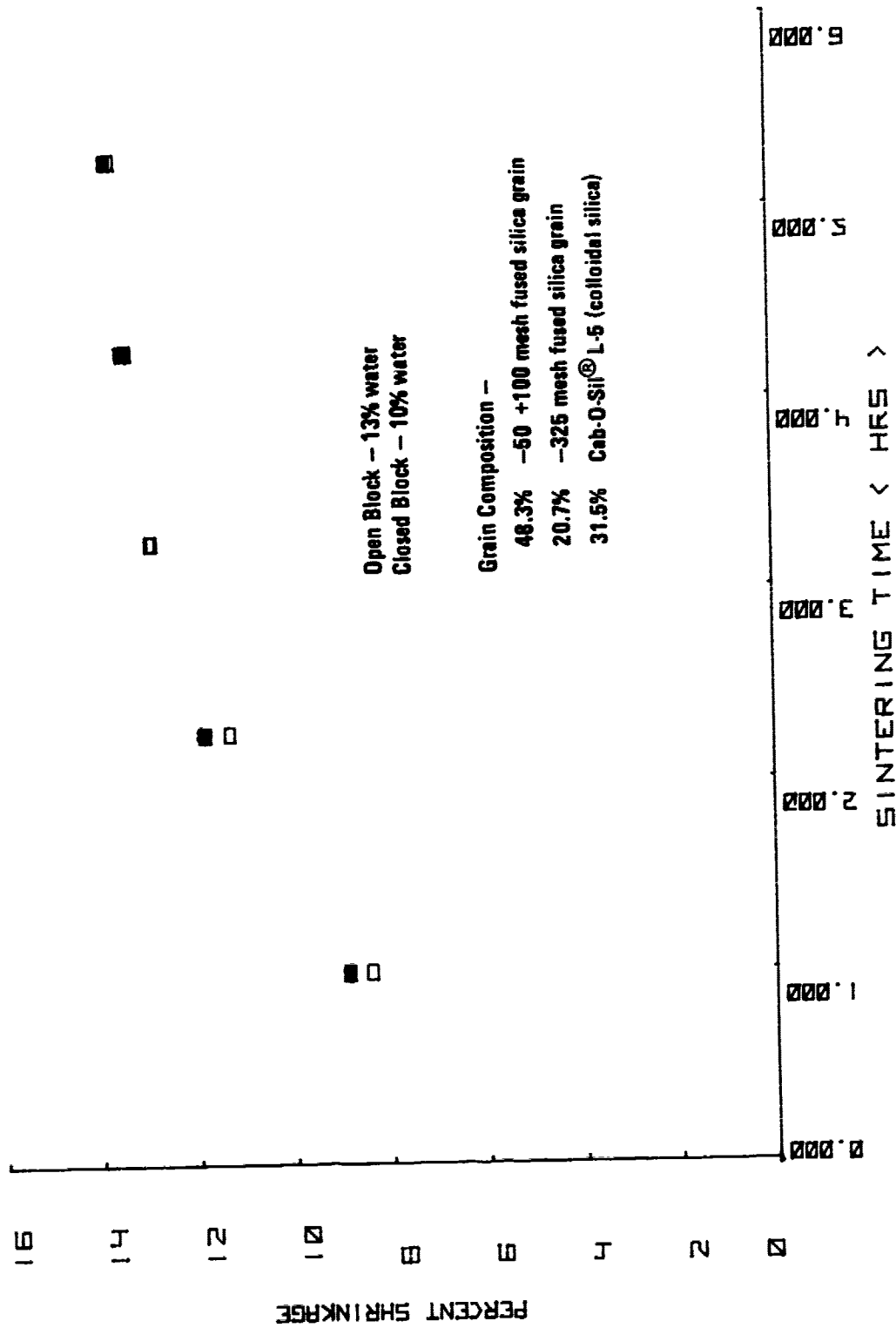


Figure 17a. Shrinkage Versus Sintering Time @ 2300°F

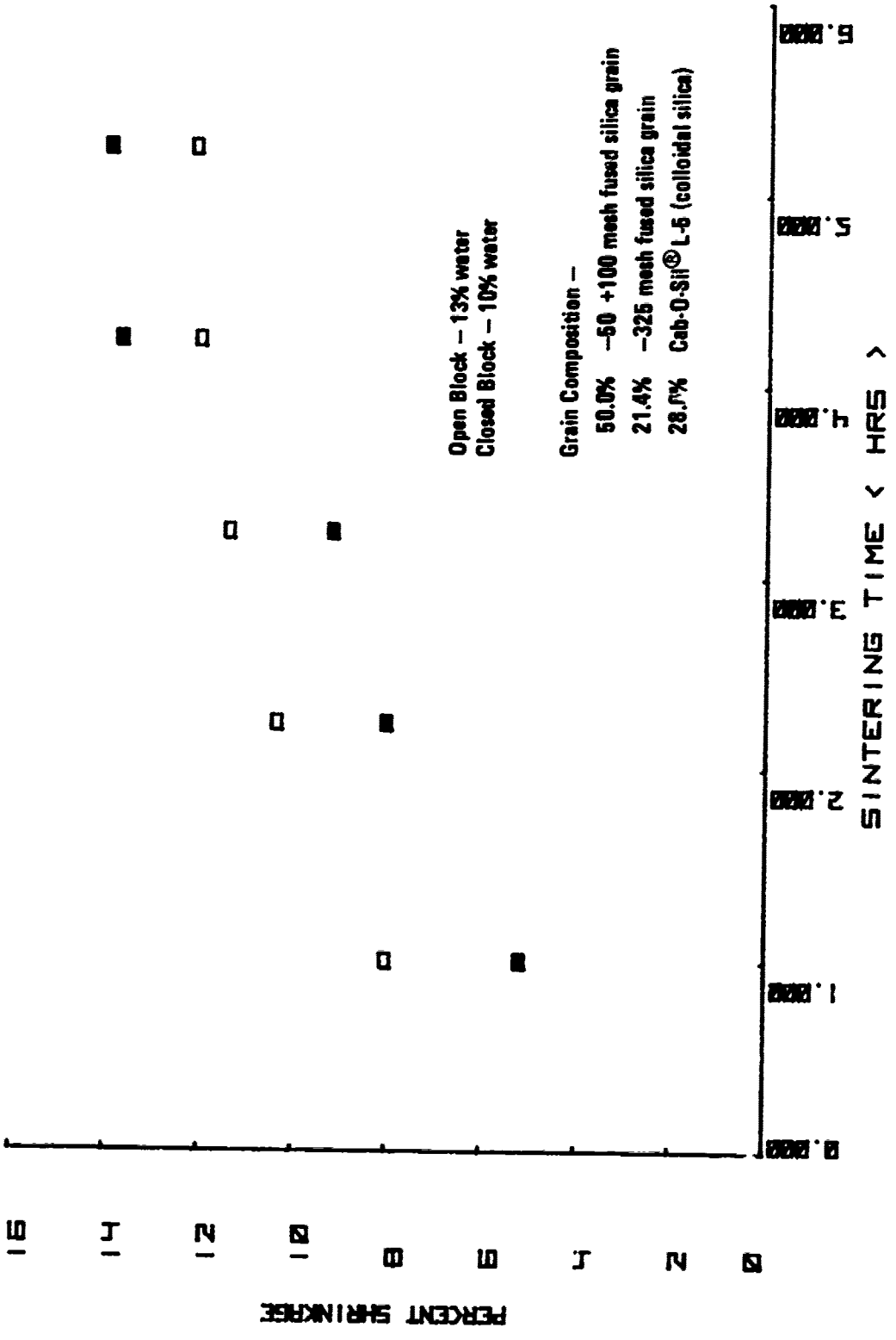


Figure 17b. Shrinkage Versus Sintering Time @ 2300°F

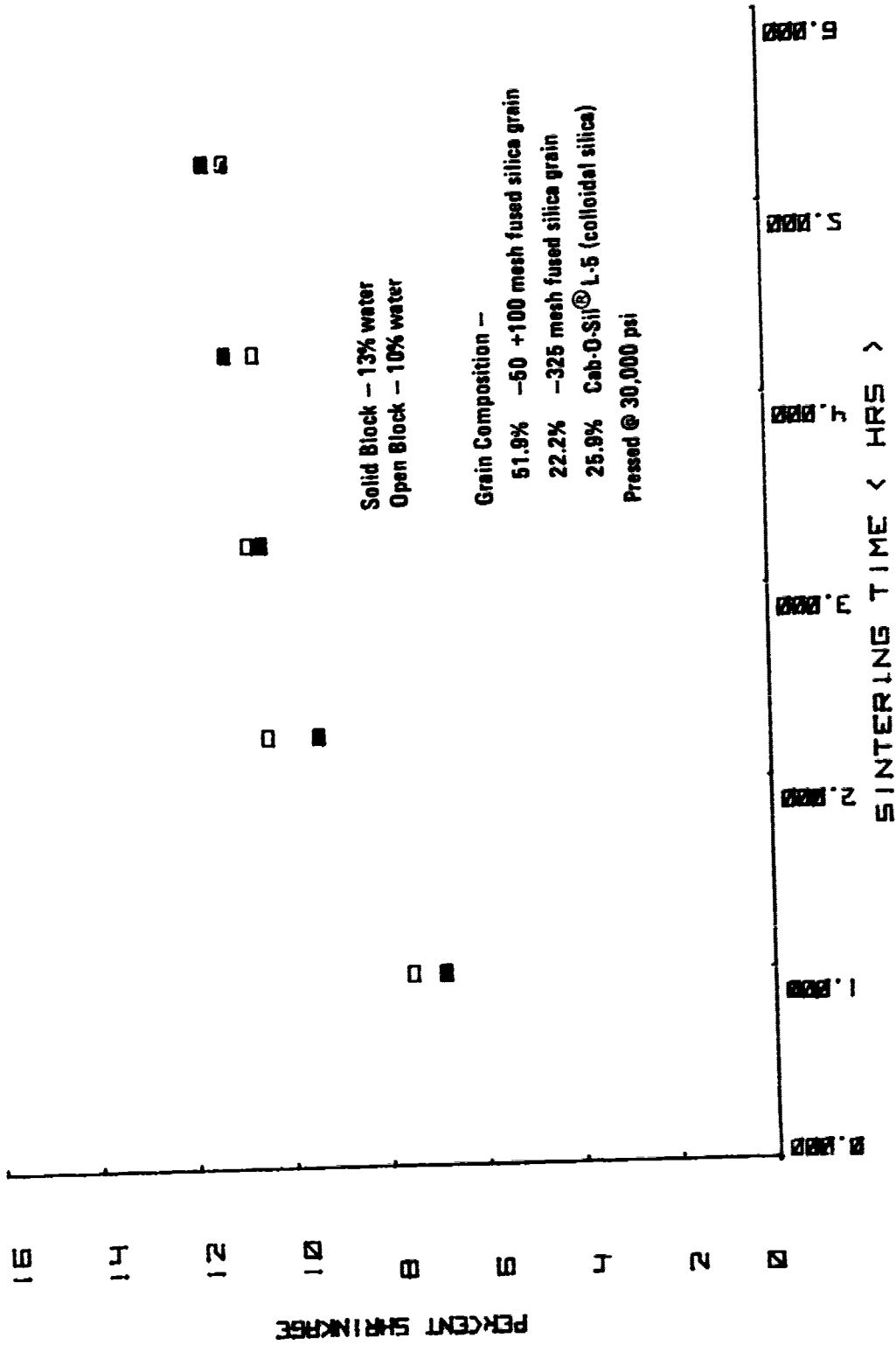


Figure 17c. Shrinkage Versus Sintering Time @ 2300°F

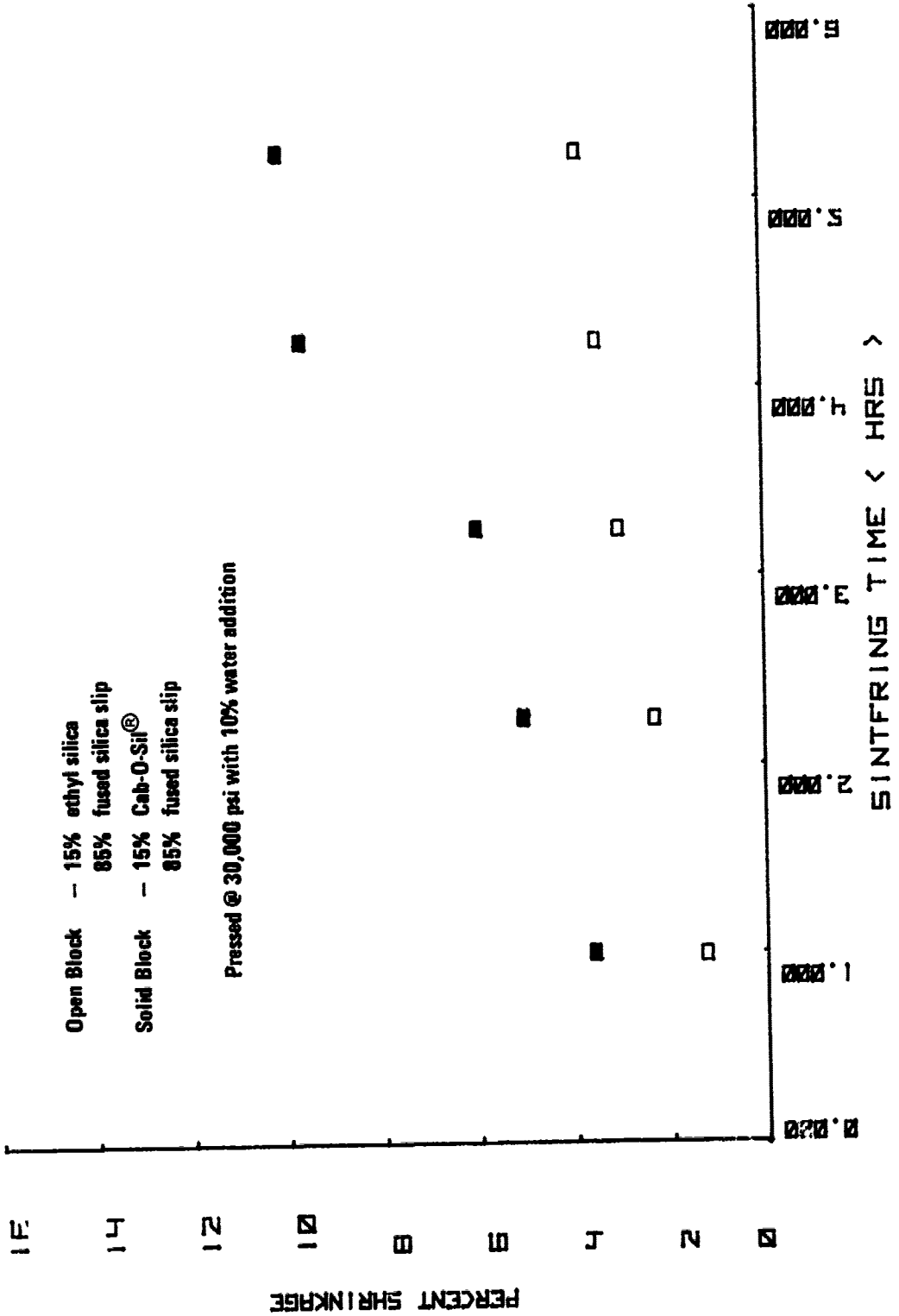
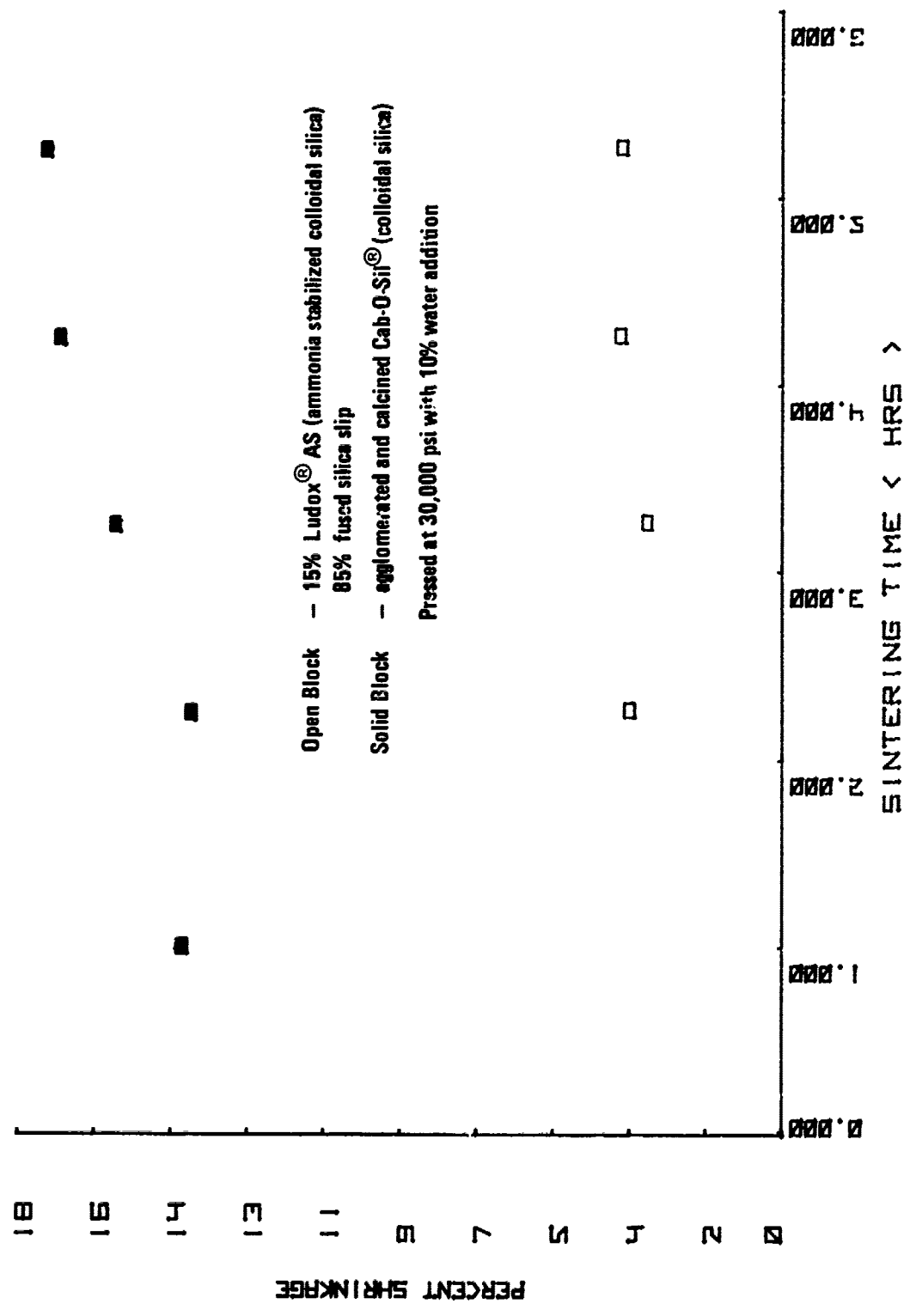


Figure 17d. Shrinkage Versus Sintering Time @ 2300° F



Open Block - 15% Ludox<sup>®</sup> AS (ammonia stabilized colloidal silica)  
 85% fused silica slip

Solid Block - agglomerated and calcined Cab-O-Sil<sup>®</sup> (colloidal silica)

Pressed at 30,000 psi with 10% water addition

Figure 17e. Shrinkage Versus Sintering Time @ 2300°F

This page intentionally left blank.

APPENDIX III

MILLING OF HIGH PURITY FUSED SILICA (SYLVANIA) CULLET

A porcelain-lined 55-gallon ball mill was cleaned by first milling 75 lbs. of -50 +100 mesh technical grade fused silica grain for approximately 20 minutes. Both the grain and grinding balls were emptied from the mill, then recharged with 100 - 150 lbs. of alumina grinding media and 50 lbs. of the high purity glass cullet. After grinding for 40 minutes the cullet was screened, giving the following particle size distribution:

<u>Mesh</u>	<u>Weight (lbs.)</u>
+50	9
-50 +100	12.5
-100 +200	11.75
-200 +325	6
-325	7
TOTAL	46.25 lbs.

This page intentionally left blank.

## APPENDIX IV

### PROCEDURE USED TO PRESS RADOME

The component list (Figure 14) and assembly procedure for the radome fabrication is as follows:

- a. Centering ring for mandrel
  - b. Aluminum cap and evacuating valve
  - c. Spacing ring
  - d. Stainless steel internal mandrel
  - e. Rubber containment bag
  - f. Perforated aluminum dam
1. The rubber containment bag (Part e) was placed in aluminum dam (Part f). The outside dimensions of the rubber bag corresponded to the inside dimensions of dam. The rubber bag extended one inch over the height of dam.
  2. The spacing ring (Part c) was placed on the dam to prevent the centering ring (Part a) from contacting the top of the rubber bag.
  3. The internal mandrel (Part d) was screwed onto the centering ring (Part a) and inserted into the rubber bag. This resulted in an open space of 1/2-inch around the surface of the mandrel. Therefore, the radome fabricated would have a 1/2-inch thick wall before pressing.
  4. The radome was packed by flowing powder through the openings in the centering ring and by a combination of tapping and vibrating the whole assembly. The process was continued until the powder level reached the edge of the internal mandrel base.
  5. The centering ring was unscrewed and both it and the spacing ring were removed from the assembly (The internal mandrel remaining in the rubber mold).

6. The aluminum cap (Part b) was placed on top of the internal mandrel and inside the rubber bag. The cap was 1/2-inch in thickness with a groove and a O-ring around its circumference in order to obtain a good seal with the rubber bag. A hose clamp was placed on the outside of the rubber bag (at the location of the cap) and tightened.
7. Using the needle valve on the cap, the system was evacuated and the valve closed.
8. The assembly (aluminum dam, rubber bag, internal mandrel and cap) was lowered in the cavity of the isostatic press.
9. After pressing, the hose clamp, cap and rubber bag were removed and the internal mandrel taken out of the radome.

## REFERENCES

1. Kingery, W. D., Introduction to Ceramics, John Wiley and Sons, Inc., New York, 1960.
2. Corbett, W. J., A. T. Sales, J. D. Walton, Jr., Improving the Mechanical Properties of Slip-Cast Fused Silica by Fibrous Reinforcement, Final Report, Contract No. 16-2092, Sandia Corporation, Albuquerque, New Mexico, prepared by Georgia Tech Engineering Experiment Station, 1965.
3. Harris, J. N., et al., Ceramic Systems for Missile Structural Applications, Final Report, Contract N00017-70-C-4438, Naval Ordnance Systems Command, prepared by Georgia Tech Engineering Experiment Station, June 1972.
4. Adams, Edward F., "Slip-Cast Ceramics," in High Temperature Oxides, Vol. 4, Allen M. Alper, ed., Academic Press, New York, 1971.
5. Murray, P., et al., "The Preparation of Dense Thoria Crucibles and Tubes," Trans. Brit. Ceram. Soc. 55, (3) 191-201, 1956.
6. Pivinskii, Yu E., "Increasing the Density of Particle Packing in Forming Ceramics," Glass and Ceramics: Russia, 26, (9), 538-542, 1969.
7. Pivinskii, Yu E., "Processes in Producing Slip and Casting Quartz Ceramics," Refractories: Russia, 36, (7), 462-471, 1971.
8. Lewis, H. D., A. Goldman, Theoretical Small Particle Statistics: A Summary of Techniques for Data Analysis with Recent Developments in Data Comparison, Notation, and Mixture Theory, Report No. LA-3656, Los Alamos Scientific Laboratory, 1967.
9. Murphy, C. A., et al., High Temperature Low-Loss Dielectric Material Studies, Sub-Contract 18-15239 to N00030-66-C-0186, Lockheed-Missiles and Space Company, prepared by Georgia Tech Engineering Experiment Station, 1968.
10. Birks, J. B., J. H. Schulman ed., "Electrophoretic Deposition of Insulating Materials," in Progress in Dielectrics I, Heywood and Company Ltd., London, 1959.

11. Willbanks, C. E., The Ablation of Slip-Cast Fused Silica, Thesis Ph.D.), Georgia Tech, 1967.
12. Hausner, H. H., K. H. Roll, P. K. Johnson, Editors, Vibratory Compacting Principles and Methods, Plenum Press, 1967, p 209.
13. Harris, J. N., E. A. Welsh, J. H. Murphy, Fused Silica Design Manual, Technical Report No. 4, Contract No. N00017-70-C-4438, Naval Ordnance Systems Command, prepared by Georgia Tech Engineering Experiment Station, 1972.
14. Perry, R. H., C. H. Chilton, S. D. Kirkpatrick, Perry's Chemical Engineers Handbook, McGraw Hill, 1963, pp 20-57.
15. Marshall, W. R., Atomization and Spray Drying, Chem. Eng. Monogram Series No. 2, 1954.
16. Harris, J. N. and E. A. Welsh, "High-Strength, Broadband, Light-weight Silicon Oxide Radome Techniques," AFAL-TR-69-103, April 1969.

Unclassified

Security Classification

DOCUMENT CONTROL DATA - R & D

Security classification of title, body of abstract and indexing annotation must be entered when the overall report is classified

1. ORIGINATING ACTIVITY (Corporate author) Georgia Tech Research Institute Georgia Institute of Technology Atlanta, Georgia 30332		2a. REPORT SECURITY CLASSIFICATION Unclassified	
		2b. GROUP	
3. REPORT TITLE AN INVESTIGATION OF FUSED SILICA COMPOSITES FOR IMPROVEMENT OF ABLATION AND RAIN EROSION RESISTANCE, AND AN ALTERNATE METHOD FOR MANUFACTURE OF FUSED SILICA RADOMES			
4. DESCRIPTIVE NOTES (Type of report and inclusive dates) Final Technical Report - 7 December 71 to 7 February 73			
5. AUTHOR(S) (First name, middle initial, last name) Earle A. Welsh, Stanley A. Byers, Joe N. Harris			
6. REPORT DATE December 1972		7a. TOTAL NO. OF PAGES 94	7b. NO. OF REFS 16
8a. CONTRACT OR GRANT NO DAAH01-72-C-0400		9a. ORIGINATOR'S REPORT NUMBER(S) A-1381	
b. PROJECT NO		9b. OTHER REPORT NO(S) (Any other numbers that may be assigned this report)	
c.			
d.			
10. DISTRIBUTION STATEMENT Distribution limited to U.S. Government agencies only; other requests for this document must be referred to U.S. Army Missile Command (AMSMI-RSM). TJK 23 APR 1973			
11. SUPPLEMENTARY NOTES		12. SPONSORING MILITARY ACTIVITY Ground Equipment & Materials Directorate U.S. Army Missile Command Redstone Arsenal, Alabama 35809	
13. ABSTRACT The objectives of this program are to develop composite materials based on slip-cast fused silica which have a higher degree of rain erosion resistance and ablation resistance than fused silica itself, and to develop a method other than slip casting for fabrication of rebonded fused silica radomes.  Task I of this program studies the effects of small additions of SiC and Si <sub>3</sub> N <sub>4</sub> on the ablation and rain erosion resistance of slip-cast fused silica. The best composites were in the range of 10 per cent SiC and 10 per cent Si <sub>3</sub> N <sub>4</sub> . Ablation resistance was improved with both additives, but resistance to rain erosion did not show any improvement under the test conditions used.  Task II of this program evaluated isostatic pressing as an alternate radome forming method. Radome shapes were pressed; however, physical properties of the pressed fused silica powders were less than those of slip-cast items. Work so far indicates that the isostatic pressing process has potential, but that further development is still needed.			

Unclassified

Security Classification

14 KEY WORDS	LINK A		LINK B		LINK C	
	ROLE	WT	ROLE	WT	ROLE	WT
Fused Silica, Slip-Cast						
Fused Silica, Composite						
Fused Silica, Isostatically Pressed						